EROSION OF METAL PIPE BY SOLID PARTICLES ENTRAINED IN WATER

by

DOREEN JOAN BLANCHARD

B.E., The Cooper Union for the Advancement of Science and Art
(1979)

SUBMITTED IN PARTIAL FULFILLMENT
OF THE REQUIREMENTS FOR THE
DEGREE OF

MASTER OF SCIENCE

at the

MASSACHUSETTS INSTITUTE OF TECHNOLOGY

January 1981

Signature of Author Doreen J. Blanchard
Department of Mechanical Engineering, January 30, 1981

Certified by Peter Griffith
Peter Griffith, Thesis Supervisor

Certified by Ernest Rabinowicz
Ernest Rabinowicz, Thesis Supervisor

Accepted by W.M. Rohsenow
Chairman, Departmental Graduate Committee

EROSION OF METAL PIPE BY SOLID PARTICLES ENTRAINED IN WATER

by

DOREEN J. BLANCHARD

Submitted to the Department of Mechanical Engineering on January 30, 1981 in partial fulfillment of the requirements for the Degree of Master of Science.

ABSTRACT

The erosion process of a 90 degree pipe elbow is investigated with the specific goals of determining the magnitude and location of the maximum wear point. A two-dimensional, theoretical model of the erosion process which tracks the particle trajectories and then calculates the wear at impingement, is inaccurate in its prediction of the erosion profile. Unaccounted for secondary flows are believed to be the cause of the discrepancy. Erosion tests on electroplated, 1 inch I.D. elbows are made using particle sizes which vary by over an order of magnitude. The results indicate an unexpected consistency in the location of maximum wear for an elbow whose R/D value is 1.5. The average angle, ϕ, which locates the point of maximum erosion, is determined to be 85 degrees, measured from the horizontal axis. The average wear coefficient, K_e, is found to be .011. The mitre bend is tested as a lower bound for the R/D value of an elbow. The resulting wear pattern substantiates the strong effect of secondary flows on the erosion profile. A wear coefficient of .057 is calculated. A further erosion test is performed with a more gradual bend curvature (R/D = 5.0) and a K_e of .028 is determined. The maximum erosion point occurs at an angle, ϕ, of 75 degrees. Finally, a simple, conservative technique is outlined to predict the erosion depth at the maximum wear point of a 1 inch I.D., 90 degree elbow.

Thesis Supervisors: Peter Griffith
Ernest Rabinowicz
Title: Professors of Mechanical Engineering

ACKNOWLEDGEMENTS

I wish to express my sincere gratitude to Professor P. Griffith for his guidance and continuous encouragement throughout the course of this research. I would also like to thank Professor E. Rabinowicz for his good advice and valuable suggestions offered on numerous occasions. Furthermore, I very much appreciate the invaluable assistance provided by members of the technical staff of the Experimental Projects Lab. Finally, I am especially grateful to Ms. Prudy Young for typing this report.

Funding for this project was provided by the Mobil Oil Company.

TABLE OF CONTENTS

TABLE OF CONTENTS (Cont.)

INTRODUCTION

Erosion, the process of metal removal by solid particle impact, is a widespread problem throughout industry. Conduits, whose conveying media contain entrained particles, experience costly erosion. In particular, in the oil industry, entrained abrasive sand particles are carried with the oil up the well string, causing wear of the oil pipeline. Where an inline fitting or weld seam appears, the erosion is greatly enhanced. One fitting of interest, the elbow, will be the subject of investigation in this report.

Before a study is undergone of the erosion of pipe elbows by solid particles entrained in a liquid, it is important to examine the problem and define more exactly the goals to be achieved. Although a prediction on the total amount of wear that an elbow will experience under certain operating conditions is important, more important is the location of maximum wear and the erosion rate occurring at that point. This is the key in determining the useful life of an elbow.

I. Finnie[1] developed a theory for the mechanism of erosion which predicts the wear produced by a single particle impingement upon a ductile metal. The model correlates the erosion rate with the metal hardness and the particle's mass, velocity, and angle of impact. The wear rate is shown to vary with the square of the velocity and inversely with the metal hardness. Seeing how the velocity plays so important a role in the process, a good prediction of the

wear experienced by an elbow must rely upon an accurate value for the particle velocity.

With this in mind, a two-dimensional, theoretical model is developed as a tool in predicting the erosion of a 90 degree elbow. It should be mentioned that a two-dimensional model will adequately describe the erosion occurring only along the symmetrical axis of the elbow; however, this axis does experience the worst erosion in the entire elbow.

The first step includes developing the equations of motion of the solid particles, thereby determining the particle trajectories and velocities upon impact with the ell wall. An accurate description of the particle velocity is contingent upon a valid velocity profile of the fluid passing through the elbow. Therefore, various velocity profiles are considered in hopes of obtaining the most correct approximation to the actual three-dimensional case. It will be seen that none of the ideal velocity profiles accurately predict the actual point of maximum erosion because no ideal theory has a good secondary flow model.

The next step in the model uses the information obtained about the particle impact (i.e., velocity, location, angle of impact) to estimate the wear due to a single collision. A modified version of Finnie's wear equation is employed in this step. Next, an averaging scheme, which takes into account the total number of particles entering the elbow, predicts the number of collisions occurring at a

given point along the wall. Knowing the wear incurred by each collision, a profile of erosion is obtained.

Of course, a theoretical model which is not supported with experimental evidence is of limited value. Therefore, erosion experiments are performed employing a technique devised to precisely locate the point of maximum erosion. Various sand particle sizes are tested as well as three different elbow geometries: a mitre bend, an R/D value of 1.5, and an R/D value of 5.0. Eventhough these do not cover all possible geometric configurations of a pipe elbow, it is hoped that they are broad enough in range to allow predictions to be made on the erosion occurring in elbows of other sizes.

II. MODEL OF EROSION OF PIPE ELBOWS

(1) Particle Flow Through A 90 Degree Elbow

In the theoretical analysis of the abrasive erosion of a pipe elbow, it is necessary to calculate the trajectories of the entrained solid particles. From this, information is obtained required to compute the erosion profile along the bend. The particle trajectories are developed by integrating the two-dimensional equations of motion of the particle. The equations of motion are written by simply performing a force balance on the particles. For a solid particle entrained in a liquid, buoyancy and drag are the only two forces acting on it. If the abrasive particle is assumed spherical, the drag coefficient can be expressed by the following empirical correlation[2],

$$C_d = \frac{24}{Re} + \frac{6}{1+\sqrt{Re}} + 0.4 \qquad (1)$$

where the Reynolds number is given by,

$$Re = \frac{d}{\nu}\left((u-\dot{x})^2 + (v-\dot{y})^2\right)^{0.5} \qquad (2)$$

The quantities u and v are the x and y velocity components of the liquid flowing through the ell and ν is its kinematic viscosity. The particle diameter is given by d and its velocity components are $\dot{x}$ and $\dot{y}$. Using this correlation, the drag force on a solid particle may be expressed as,

$$\text{Drag Force} = 1/2\ C_d\ A_p \rho_f\ (\bar{V}_s - \bar{V})^2 \tag{3}$$

where $\bar{V}_s$ is the fluid streamline velocity vector, $\bar{V}$, the particle velocity vector, and A_p, the frontal area of the particle in the streamwise direction. The buoyancy force can be expressed as,

$$\text{Buoyancy Force} = \frac{\pi}{6} d^3(\rho_p - \rho_f)g \tag{4}$$

where ρ_p and ρ_f are the densities of the particle and the fluid, respectively. When these terms are equated to the inertial forces of the particle, the resulting expressions in two dimensions are,

x-direction:

$$\frac{\pi}{6} d^3(\rho_p + {}^1/_2\ \rho_f)\ddot{x} = 1/2\ C_d \rho_f A_p (u-\dot{x})((u-\dot{x})^2 + (v-\dot{y})^2)^{0.5} \tag{5}$$

y-direction:

$$\frac{\pi}{6} d^3(\rho_p + {}^1/_2\ \rho_f)\ddot{y} = 1/2\ C_d \rho_f A_p (v-\dot{y})((u-\dot{x})^2 + (v-\dot{y})^2)^{0.5} + \frac{\pi}{6} d^3(\rho_p - \rho_f)g \tag{6}$$

Note that the buoyancy force appears only in the y-direction equation of motion. The apparent mass effect leads to the additional term, $1/2\ \rho_f$, in the expression for particle mass.

If an appropriate fluid velocity profile through the elbow is established, these equations can be numerically solved to yield the particle trajectories and velocities. The actual velocity profile for a three-dimensional elbow is a complicated problem and a solution is not easily obtained. Therefore, for this model, three approximate, two-dimensional velocity profiles are tried in the computer analysis. It was necessary to go to these three tries because each of the earlier ones failed to give adequate results. They are detailed below.

(i) Uniform Velocity Profile

The uniform velocity profile is the first and least refined approximation made of the actual flow field through a 90 degree elbow. This profile, which is shown in Figure 1, assumes a uniform velocity across the diameter of the pipe. Using the axis orientation shown, the x and y components of velocity are,

$$u = -\frac{ky}{r} \tag{7}$$

$$v = \frac{kx}{r} \tag{8}$$

where the constant k is solved for by the boundary conditions. A short, horizontal extension at the exit of the ell has the velocity profile,

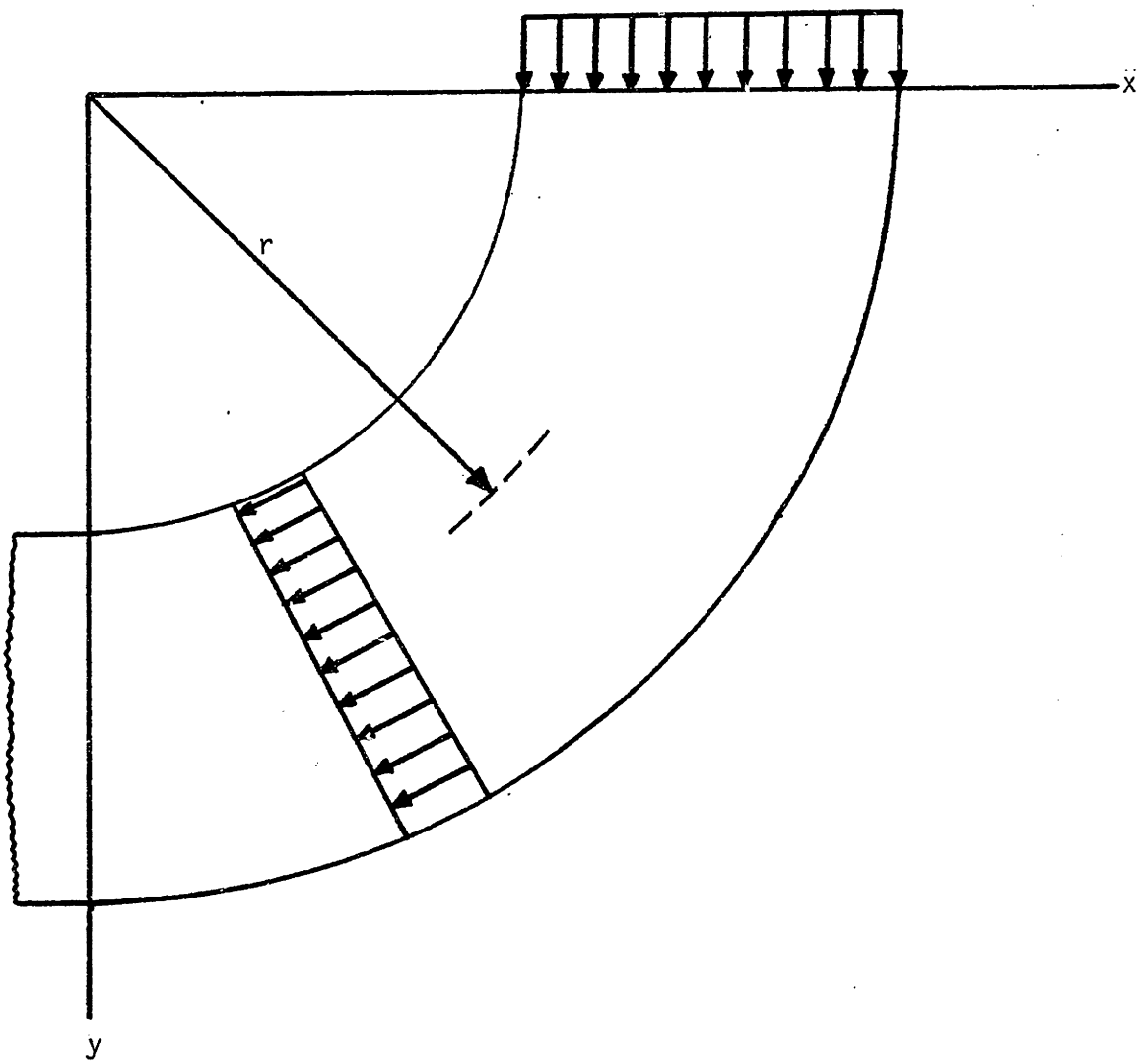

FIGURE 1 - UNIFORM VELOCITY PROFILE

$$u = -k \tag{9}$$

$$v = 0 \tag{10}$$

(ii) Hyperbolic Velocity Profile (see Appendix A)

The next profile used in the analysis, assumed at the time to be more accurate than the first, is that obtained by applying the Euler-n equation of inviscid flow to a two-dimensional elbow channel. This profile, which is pictured in Figure 2, possesses a hyperbolic shape unlike the previous profile which is linear. It is seen that the tangential velocity, V_s, is given by,

$$V_s = \frac{K}{r} \tag{11}$$

where $$K = \frac{Q}{H \ln ((R+b)/(R-b))} \tag{12}$$

and Q is the volumetric flowrate. The height H is solved for by equating the cross-sectional area with that of a one inch I.D. circular pipe. Eventhough this profile is derived for two-dimensions instead of three, it is felt that it should satisfactorily describe the flow along the main symmetric axis of the ell.

(iii) Experimental Velocity Profile

In order to get firsthand knowledge about the actual velo-

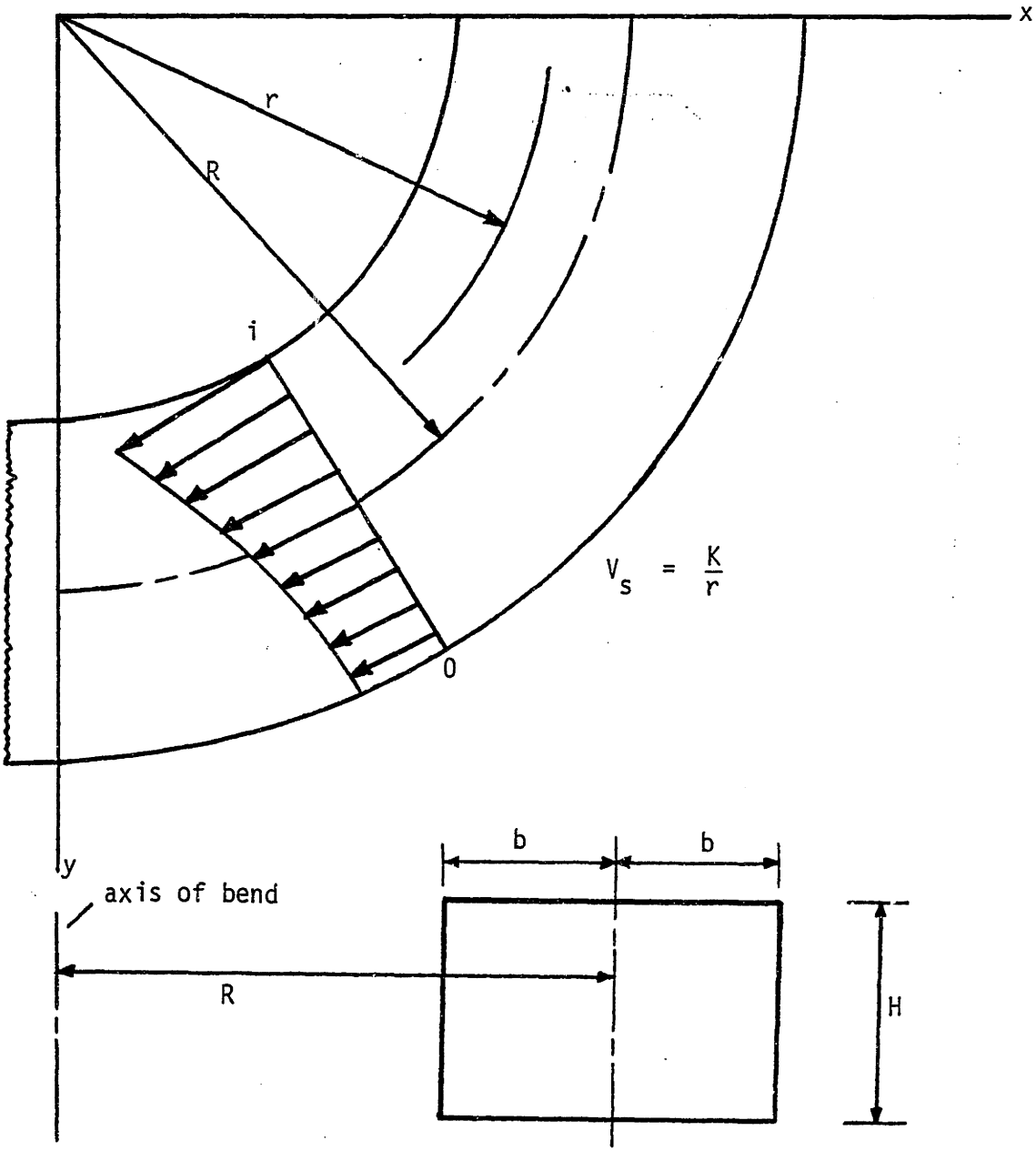

FIGURE 2 - HYPERBOLIC VELOCITY PROFILE

city profile through a one inch I.D. elbow (R/D=1.5), pitot tube measurements were taken at various points along the symmetrical diameter of the bend outlet, from inner to outer wall. The data is presented in Figure 3. The equation for the linear velocity profile shown is determined using the method of least squares. Note that although there is a boundary layer present near the pipe wall, it is ignored on the premise that the abrasive particles are much larger than the thickness of the boundary layer and would therefore be unaffected by it. A schematic of this profile in a bend is given in Figure 4.

Using the velocity profile obtained, the x and y components of the fluid velocity along the elbow are as follows,

$$u = \frac{-ky}{r} - C\,y \tag{13}$$

$$v = \frac{kx}{r} + C\,x \tag{14}$$

where, from the data, k equals 1.362 and C equals 102.39 when x, y and r are measured in meters.

The maximum velocity at a given cross-section of the elbow occurs near the outer wall, instead of the inner wall which is indicated by the hyperbolic velocity profile. This difference is due solely to the secondary flow effects which are ignored in the Euler equation solution.

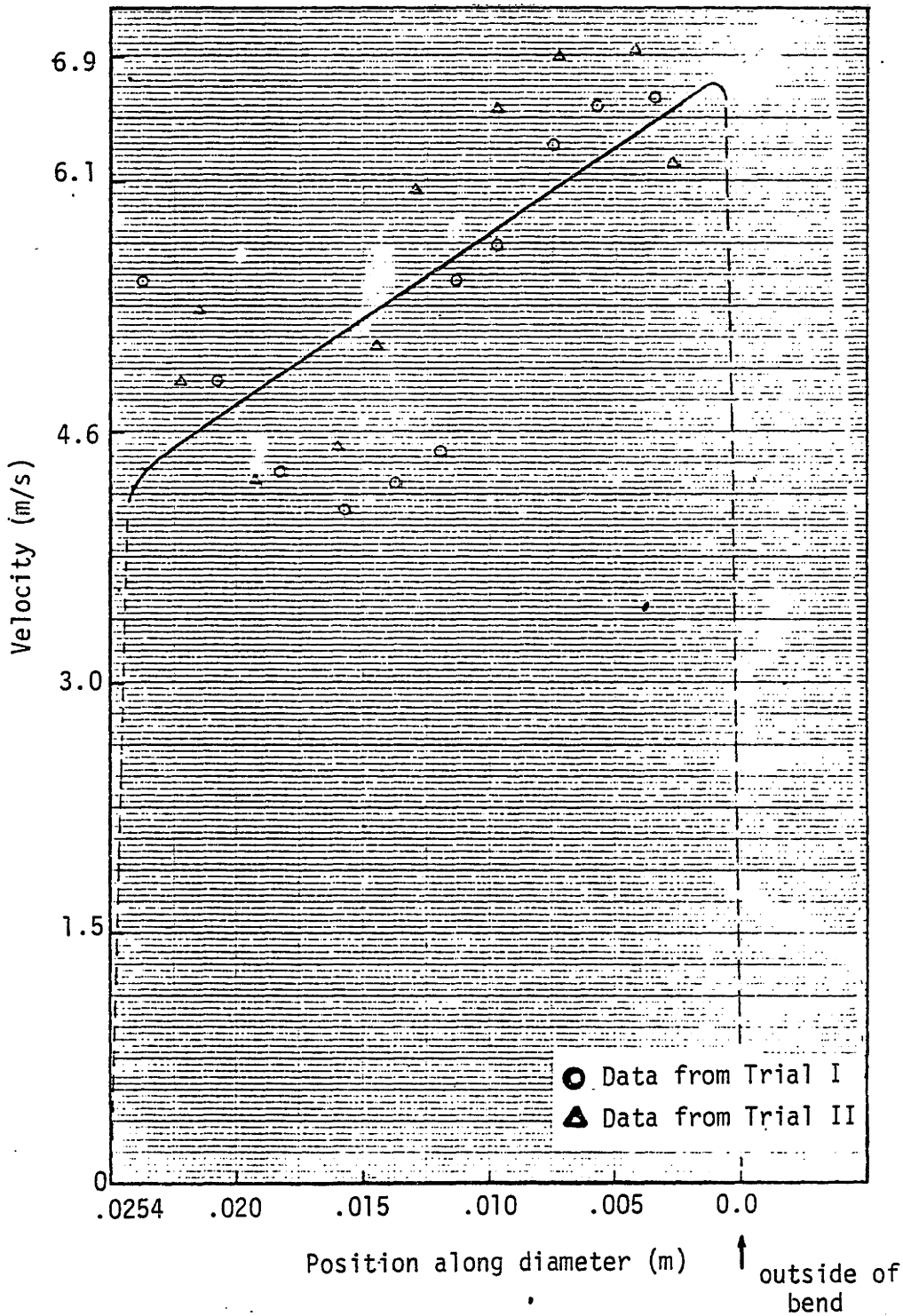

FIGURE 3 - DATA TAKEN OF VELOCITY PROFILE AT ELBOW OUTLET

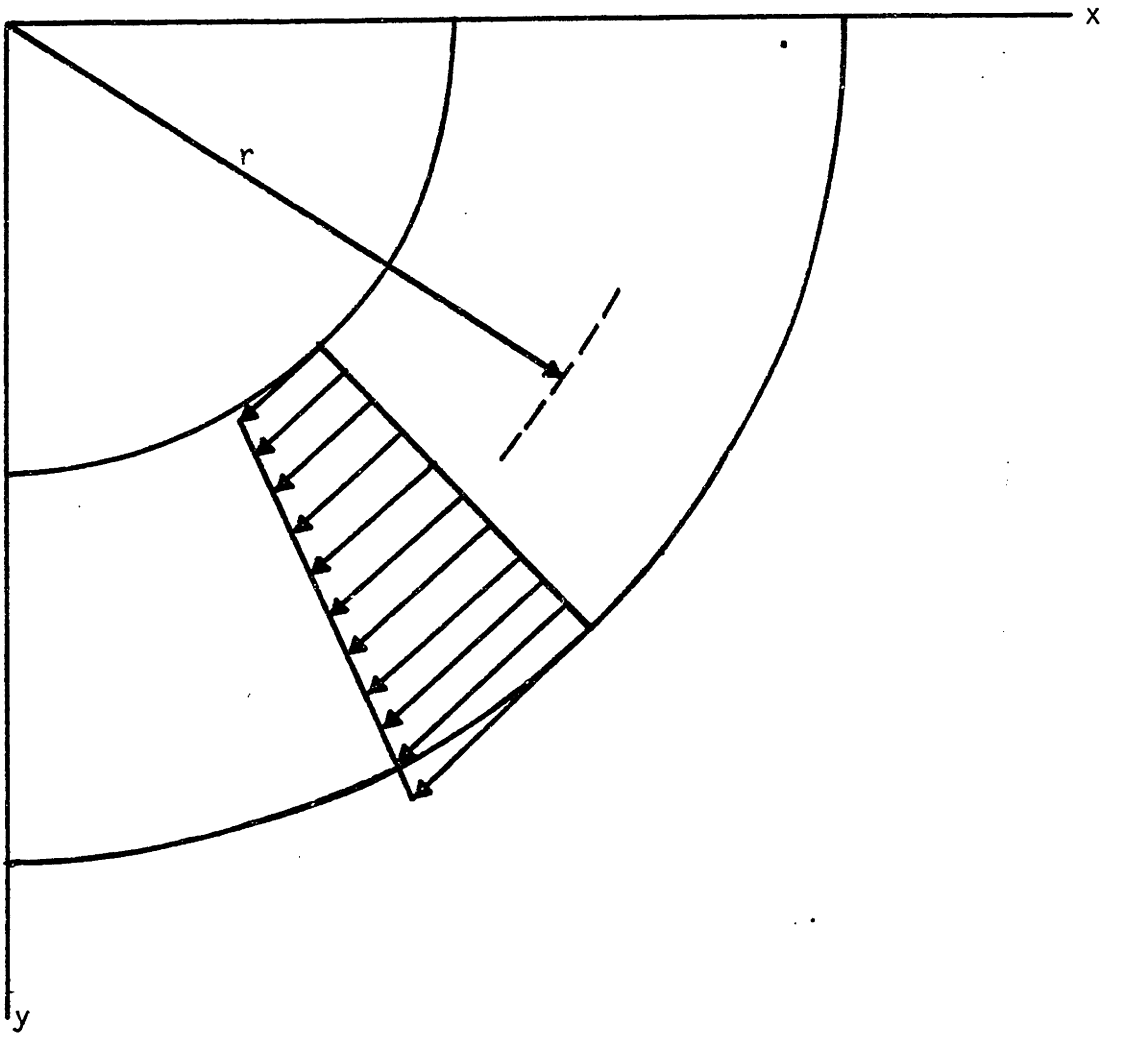

FIGURE 4 - EXPERIMENTALLY DETERMINED VELOCITY PROFILE

II. (2) Theoretical Erosion Profile Along An Elbow

(i) Erosion Equation

Until now, the emphasis has been on solving for the trajectories and velocities of the particles as they pass through the elbow. By numerically solving the equations of motion, the velocity and position of impact for a particular particle is obtainable. It is now time to utilize this information to determine the profile of erosion along the wall.

The model of erosion is based on the expression developed by I. Finnie[3] whose equation for the mass lost by a ductile metal due to particle impingement is as follows,

$$W = \frac{\rho_s m V^2}{2 p_c \, 2g} F(\alpha) \tag{15}$$

where

$$\begin{aligned} F(\alpha) &= \sin 2\alpha - 3\sin^2\alpha \qquad \alpha \leq 18.5^\circ \\ F(\alpha) &= \frac{\cos^2\alpha}{3} \qquad\qquad\quad \alpha > 18.5^\circ \end{aligned} \tag{16}$$

The angle formed by the incoming particle, of mass m and velocity V, and the tangent to the surface is α. The density of the metal is ρ_s and the penetration hardness, p_e. The expression is nearly identical to that developed by other researchers except for differences in the value of the constant (wear coefficient) in the expression and differences in the angle function. Excepting these dissimilarities, most researchers agree that wear is strongly dependent upon the

particle velocity which is usually raised to the power 2 although experimentally, values as high as 3 have been observed. Also, erosion is inversely proportional to the penetration hardness of the metal being eroded.

Another conclusion agreed upon regarding the wear expression is its dependence upon an angle function. Experimentally, the maximum erosion occurs at an angle of impact of about 20 degrees. Finnie's equation predicts this angle well, however, it fails at high angles of impingement.

Finnie's model is obtained for a particle traveling in air, not water, therefore a modification of this equation is needed to account for the apparent mass of the particle. A substitution for m, the mass of a single particle, with the assumption that it is spherically shaped,

$$m = \frac{\pi}{6} d^3 (\rho_p + {}^1/_2\, \rho_f) \tag{17}$$

will yield the following expression,

$$W = \frac{\rho_s\, \pi\, d^3 V^2 (\rho_p + {}^1/_2\, \rho_f)}{24\, p_e\, g}\, F(\alpha) \tag{18}$$

In addition, since Finnie's model predicts no erosion for an impingement angle, α, of 90 degrees, still another modification of this equation is needed. A semi-empirical correction suggested by Finnie

assumes that the weight loss at a 90 degree impingement angle is the average for all angles between 17 and 90 degrees. For angles between 17 and 90 degrees, a proportional amount, ε, in Figure 5, is added to the relative weight loss curve. The resulting weight loss curve is indicated by a dashed line. The average dimensionless weight loss for all angles between 17 and 90 degrees is calculated to be $\delta = 0.130$ (see Appendix B). Now the wear equation becomes,

$$W = \frac{\rho_s \pi d^3 V^2 (\rho_p + 1/2\ \rho_f)}{24\ p_e\ g} (F(\alpha) + \varepsilon) \tag{19}$$

where,

$$\begin{aligned} \varepsilon &= 0 && \alpha < 17^\circ \\ \varepsilon &= \frac{\delta}{73} (\alpha - 17) && \alpha \geq 17^\circ \end{aligned} \tag{20}$$

This equation, used in conjunction with the data obtained regarding the particle trajectories, enables one to calculate the wear due to a single particle impingement anywhere along the elbow wall. The velocity at each point as well as the location of the particle as a function of time is given by the solution of the governing equations of motion. Knowing the equation of the elbow wall, the angle of impingement is easily calculated.

At this point, it is possible to utilize this information to predict the profile of erosion along the elbow. The method used to calculate the depth of erosion in a flat plate by M. Benchaita[4]

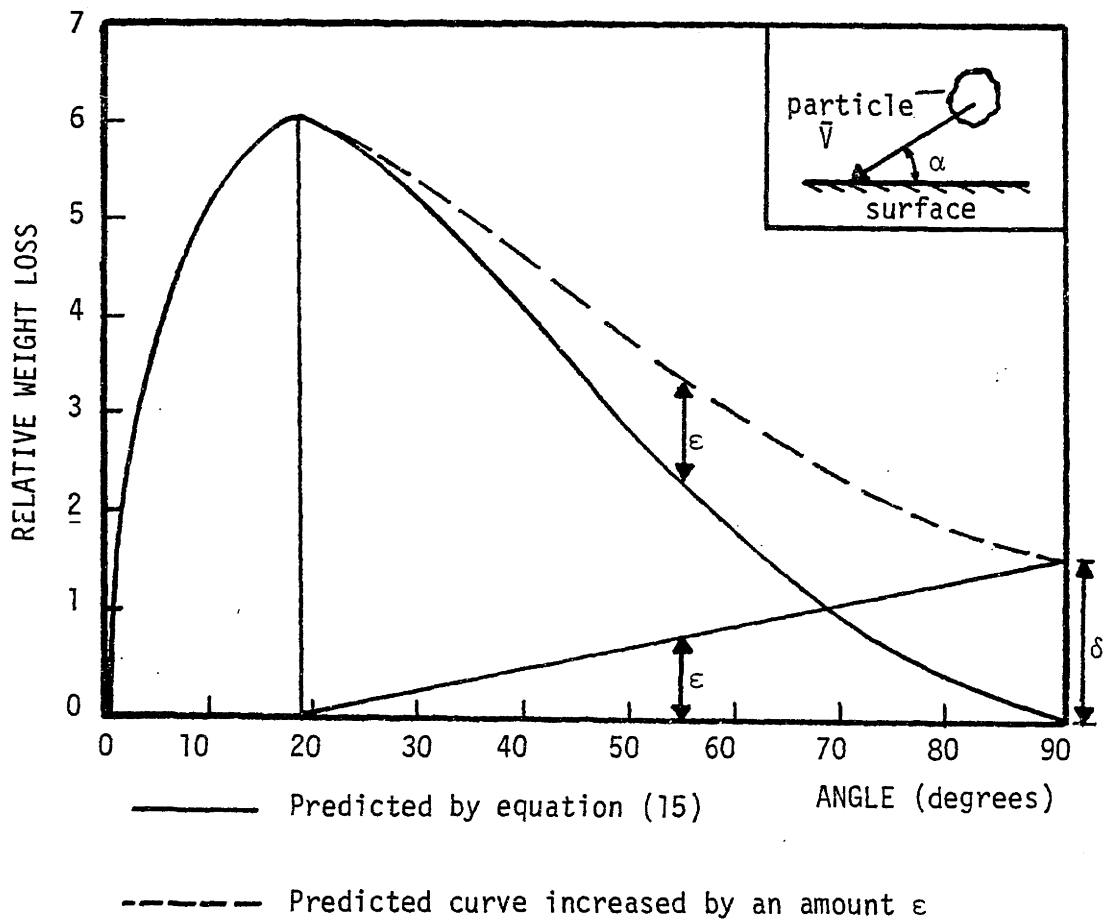

FIGURE 5 - FINNIE'S DIMENSIONLESS WEIGHT LOSS AS A FUNCTION OF IMPACT ANGLE AND THE CORRECTED CURVE

will be adapted for the case of the elbow. If γ represents the mass ratio of sand to water in the flow, then the number of particles passing through the ell entrance per unit time is,

$$N_p = \frac{6\,\gamma\,\rho_f\,V_e\,A}{\pi\,\rho_p\,d^3} = \frac{3\,\gamma\,\rho_f\,V_e\,D^2}{2\,\rho_p\,d^3} \tag{21}$$

where V_e is the mixture velocity entering the ell, and A and D are the cross-sectional area and diameter of the elbow, respectively. The depth of erosion rate is defined as the average depth eroded between the positions S_{f_j} and $S_{f_{j+1}}$ (see Figure 6) along the curve length corresponding to the x positions s_{f_j} and $x_{f_{j+1}}$. The initial x positions of these abrasives are x_{i_j} and $x_{i_{j+1}}$, with Δx_i equal to 0.1 inch. If the average value of the metal volume lost at successive impingements is divided by the length of curve between the two impingements and the width of the particle, then what is left is the depth of erosion due to a single collision. Furthermore, if this erosion depth is multiplied by the total number of particles striking that same length of wall, this gives the total depth of erosion rate. Thus, the erosion depth rate is given by,

$$h_m = N_p \frac{d\,\Delta x_i}{A} \frac{W_j + W_{j+1}}{2} \frac{1}{\rho_s\,d\,\Delta S} \tag{22}$$

where ΔS is the length along the curved wall between successive impingements,

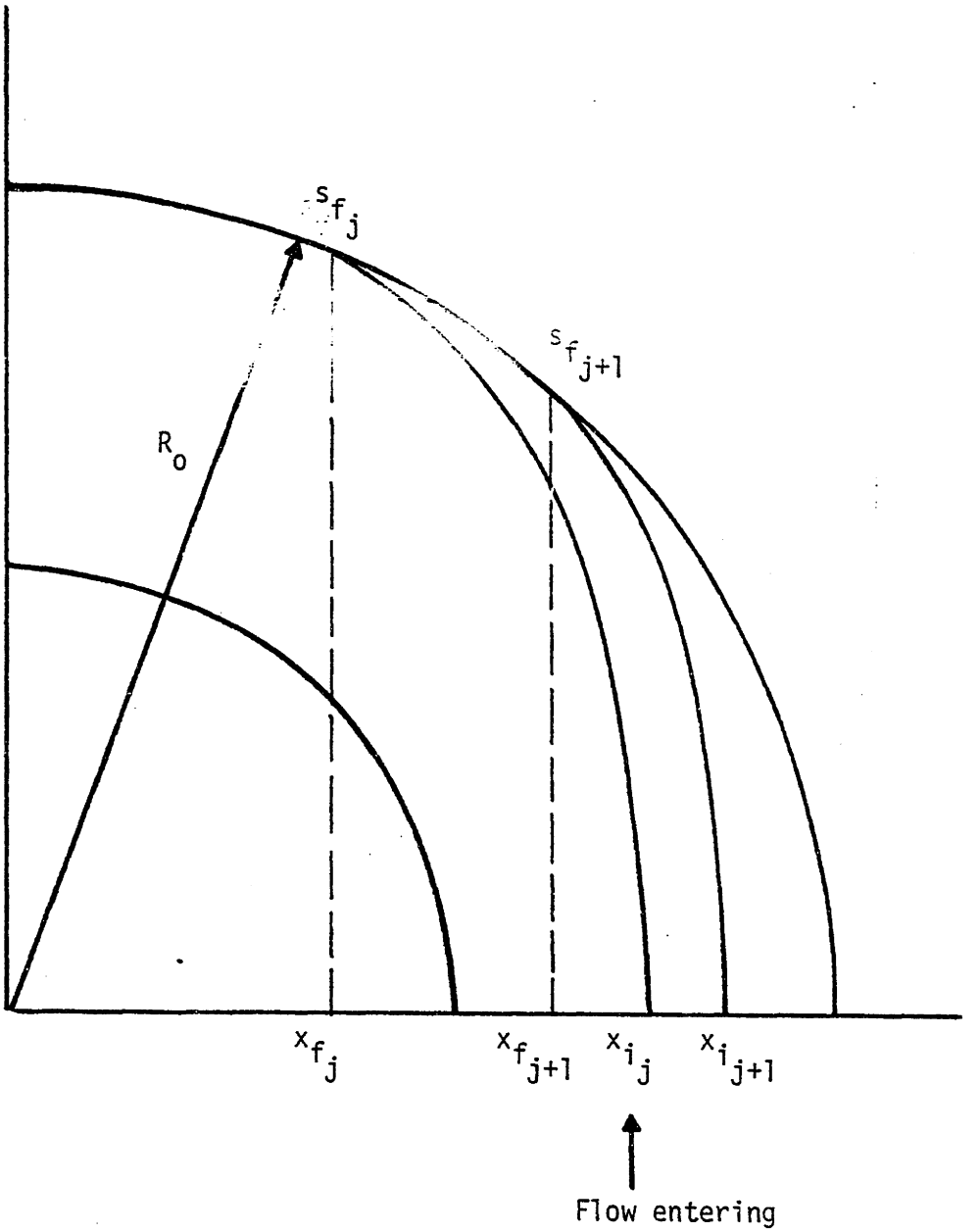

FIGURE 6 - NOMENCLATURE USED IN THEORETICAL EROSION MODEL TO CALCULATE DEPTH ERODED

$$\Delta S = R\left(\sin^{-1}(x_{f_{j+1}}/R) - \sin^{-1}(x_{f_j}/R)\right) \tag{23}$$

and R_o is the outer radius of curvature. W_j and W_{j+1} are the weight losses of the elbow at positions S_{f_j} and $S_{f_{j+1}}$, respectively.

Using the equations developed, it is possible to theoretically predict the erosion rate and erosion profile of a 90 degree elbow due to the bombardment of sand particles carried in water.

II. (2) (ii) Comparison of the Three Velocity Profiles

Before the computer simulation is performed, data pertaining to the actual experiment is sought in order that a realistic comparison between theory and experiment may be made. The first consideration is the initial conditions of the particle, namely velocity and position. The experimental setup consists of a long (1.8 m), plexiglas, vertical tube immediately preceding the entrance to the elbow. It has the same internal diameter as the ell in order to ensure a smooth transition for the flow. With this in mind, the initial particle velocity entering the elbow can be determined.

If the particle entrained in water is assumed to start from rest at the top of the plexiglas tube and accelerate down the tube under the influence of gravity and drag forces, then the particle velocity entering the elbow can be calculated using a computer simulation. The velocity of the water entering the elbow is measured to be 5.0 meters per second. Figure 7 shows the steady state velocity of 270 micron particles entrained in water at 5.0 meters per second traveling vertically down the 1.8 meter length of tubing. It is seen that a 270 micron particle achieves a speed of 5.04 meters per second in less than 0.2 meters. Similarly, 425 micron and 605 micron particles achieve steady state speeds of 5.06 and 5.09 meters per second, respectively, under identical conditions.

The three velocity profiles previously introduced are then incorporated into the erosion simulation for 270 micron sand particles

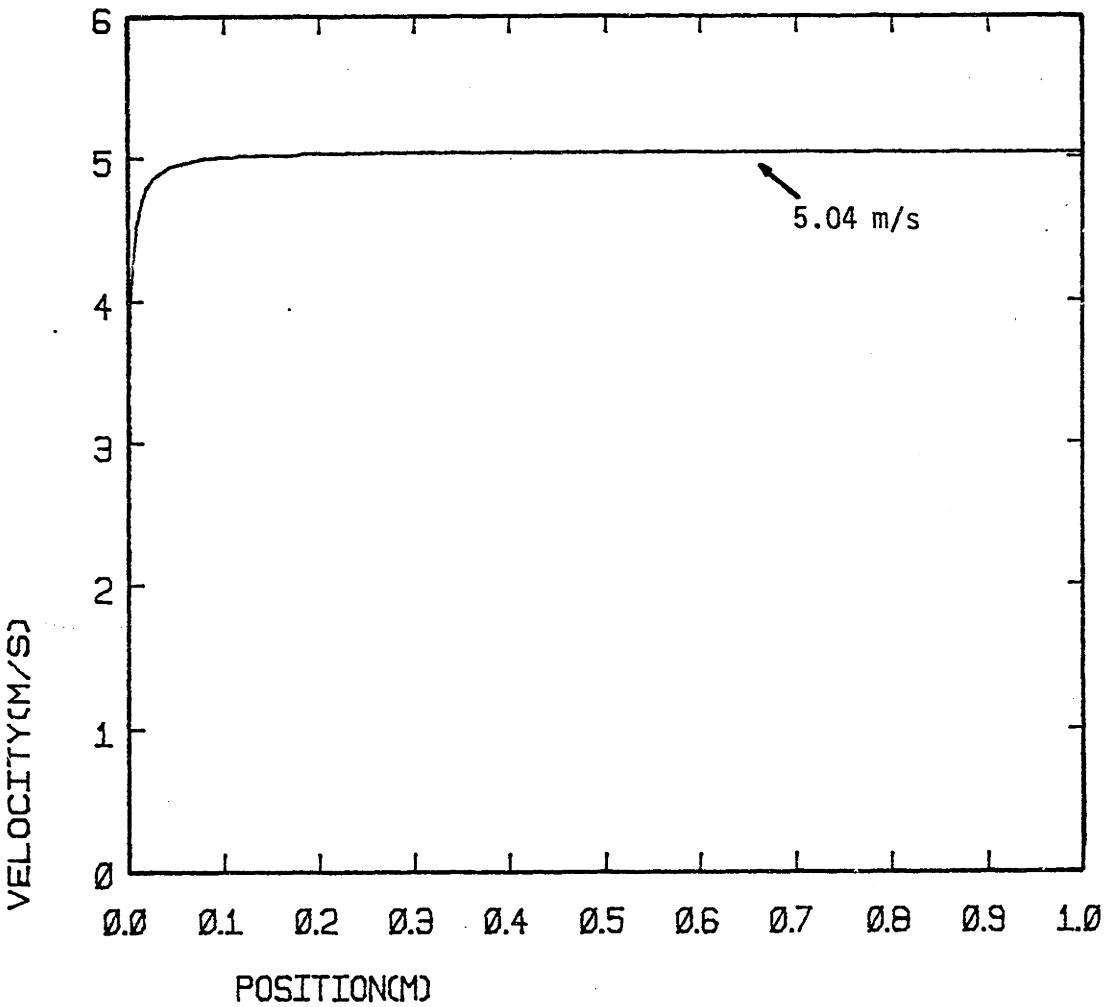

FIGURE 7 - COMPUTER SIMULATION FOR THE STEADY-STATE VELOCITY OF A 270 MICRON PARTICLE

entrained in water. The value of the sand to water mass ratio used in the simulation, γ, is taken from an actual experiment whose value for γ is 0.0164 kg/kg. The computer plotted trajectories of sand particles entering a 90 degree elbow for the cases of a uniform, hyperbolic, and experimentally determined velocity profile are shown in Figures 8, 9 and 10, respectively. A total of eleven particle trajectories are plotted for each case and are spaced at 0.1 inch intervals at the entrance to the one inch I.D. elbow. The trajectories stop upon first impact with the wall.

Below each plot of particle trajectories is a table of the particle impingement velocities. Also tabulated is the erosion depth profile which is calculated using the modified version of Finnie's wear equation (Eq. 19). Each impingement with the wall is indicated by a small circle and numbered. The wear profile is that obtained after six hours of erosion. All particles for the three cases enter with the identical initial velocity, 5.04 meters per second. The data used in the simulation is taken from an actual experiment and is listed in Table 1.

Comparing the three plots, it is difficult to differentiate between them. The corresponding points of impingement nearly coincide in all cases. However, the velocities at impact vary enough to make a substantial difference in the erosion rate. For the experimentally determined velocity profile, the impact velocity is the greatest since the higher velocities occur at the outer radii of the

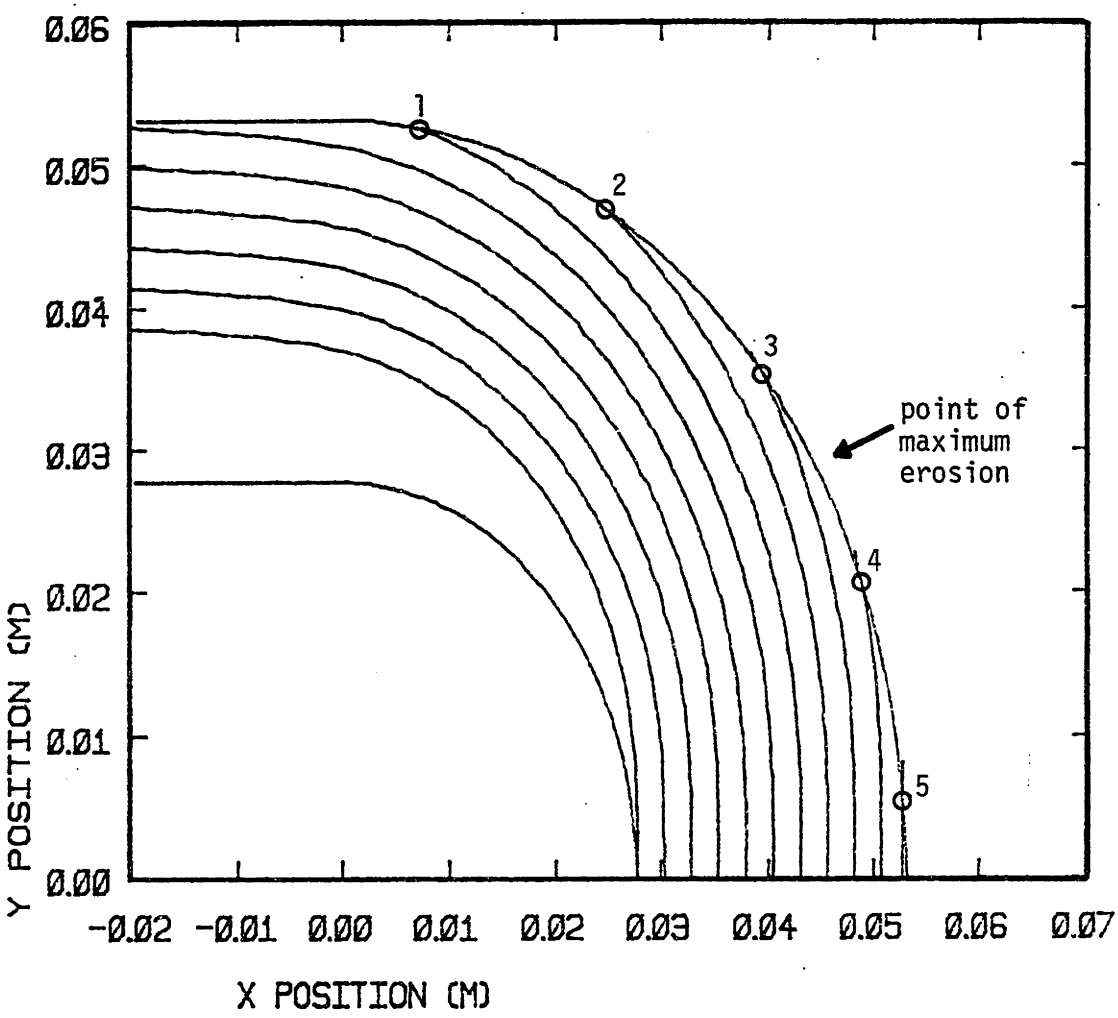

Impact No.	Velocity at Impact m/s	Erosion Depth in 6 Hrs (10^{-4}m)	Normalized Erosion Depth
1	4.95	3.96	.96
2	4.95	3.95	.96
3	4.95	4.12	1.00
4	4.98	3.40	.83
5	5.02		

FIGURE 8 - UNIFORM VELOCITY PROFILE COMPUTER SIMULATION FOR 270 MICRON PARTICLES

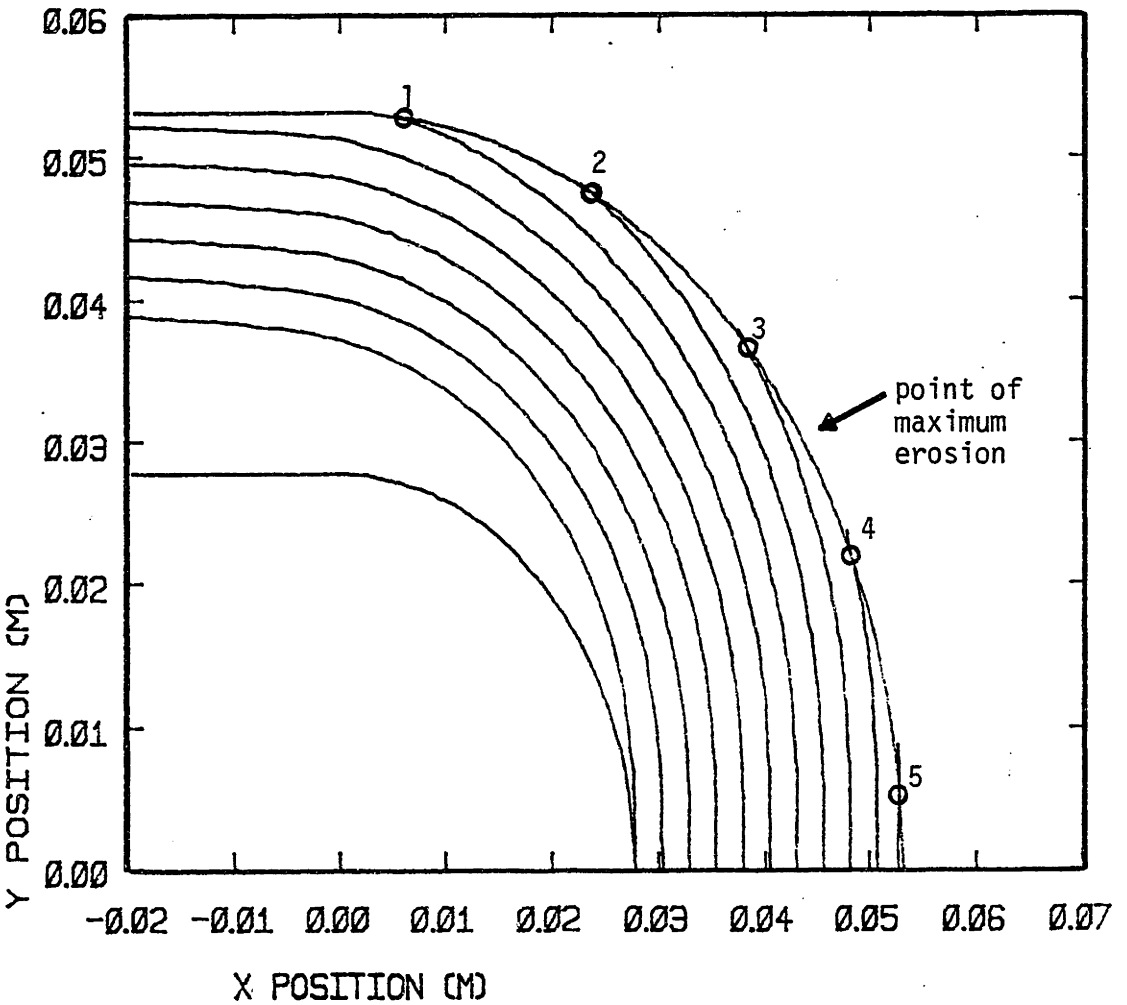

Impact No.	Velocity at Impact (m/s)	Erosion Depth in 6 Hrs. (10^{-4}m)	Normalized Erosion Depth
1	3.71		
		2.15	.96
2	3.71		
		2.16	.96
3	3.72		
		2.25	1.00
4	3.76		
		1.96	.87
5	4.06		

FIGURE 9 - HYPERBOLIC VELOCITY PROFILE SIMULATION FOR 270 MICRON PARTICLES

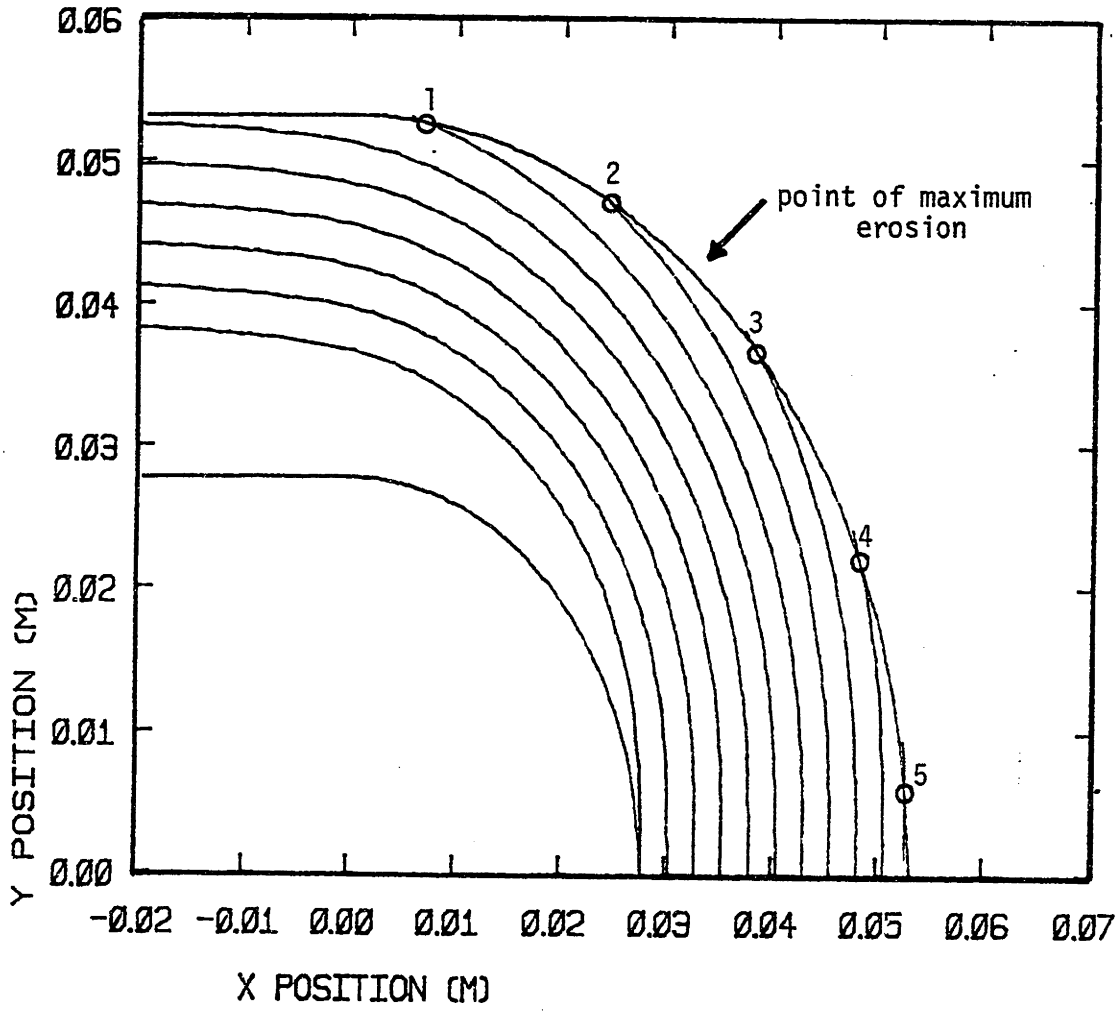

Impact No.	Velocity at Impact (m/s)	Erosion Depth in 6 Hrs. (10^{-4}m)	Normalized Erosion Depth
1	6.61		
		6.74	.86
2	6.59		
		7.82	1.00
3	6.61		
		7.29	.93
4	6.58		
		5.39	.69
5	6.28		

FIGURE 10 - EXPERIMENTALLY TESTED VELOCITY PROFILE SIMULATION FOR 270 MICRON PARTICLES

TABLE 1 - DATA USED IN COMPUTER SIMULATIONS FOR 270 MICRON PARTICLES

Particle size	2.70×10^{-4} m
Sand density	2500 kg/m^3
Water density	998.2 kg/m^3
Water velocity entering elbow	5.0 m/s
Particle velocity entering elbow	5.04 m/s
Water viscosity	9.75×10^{-7} m^2/s
R/D of elbow	1.5
Metal density	9711.5 kg/m^3
Metal hardness	107.5×10^6 kg/m^2
γ	0.0164 kg/kg
Time of erosion	6 hrs.

bend. The opposite is true for the hyperbolic velocity profile case which due to its small velocities, experiences the least erosion.

In reference to the point of maximum erosion, it is interesting to note that although all three velocity fields predict a nearly uniform erosion profile (i.e., no maximum or minimum), two of the cases predict a slight maximum wear point between points 3 and 4 in Figures 8 and 9. The last one, the experimental velocity profile, predicts a slight maximum between points 2 and 3. The normalized values of the erosion depths are also listed under each figure for a comparison.

The results of this theoretical prediction of erosion for a copper elbow are later compared to the results taken from an erosion experiment performed under identical conditions.

It should be noted that this computer simulation predicts an erosion profile based upon the fact that each particle impacts the wall only once. It may actually happen that after the initial impact, the particle travels a bit further and then impacts the wall again. If this were the case, then the point of maximum erosion would be shifted downstream of the point predicted by the model. The distance shifted would probably not be too large since each successive impingement would result in a decreased kinetic energy of the particle.

III. EROSION EXPERIMENT

(1) Experimental Setup And Procedure

The primary objective behind carrying out an erosion experiment is to gain insight into what actually happens when a fluid entrained with abrasive particles flows through a ductile metal pipe elbow. No theory, no matter how precise and informative, can ever replace firsthand evidence of the phenomenon under question. With this in mind, various erosion tests are run with a few characteristically sized elbows. From the results, it is hoped that information regarding the erosion of a broader range of sizes may be acquired.

The test rig for the erosion experiment is shown in Figure 11. Basically, the system circulates a water and sand mixture in a closed cycle. Water and a measured quantity of sand nearly fill a 42 gallon barrel which is mechanically stirred with a double paddled stainless steel stirrer. The sand is sifted to the desired size using an agitating sifter. Several sieves are vertically stacked on the sifter in order of decreasing sieve opening. The sand which falls through the upper sieve, but is caught by a lower sieve, is assumed to have a particle size of approximately the average of the two pore sizes. In this experiment, sand particle sizes of 270, 425, 605, and 1200 microns are used as abrasives to erode 90 degree, copper elbows. In addition, silicon carbide (carborundum) particles which measure 95 microns are also used to induce abrasive erosion. The stirrer prevents sand particle settling and thereby maintains a homogeneous mixture which enters the pump.

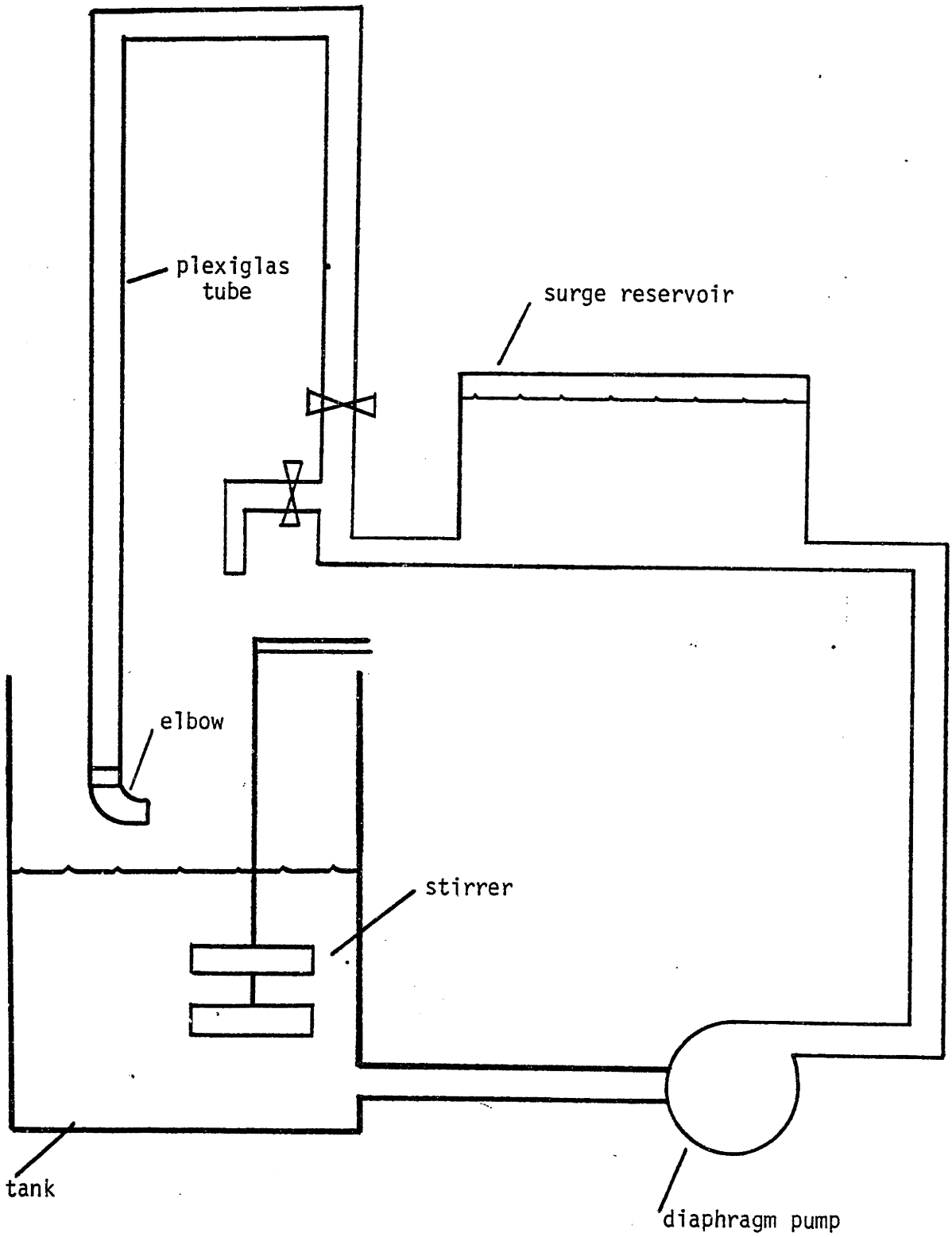

FIGURE 11 - TEST SETUP

A diaphragm pump takes the sand/water mixture from the tank and pumps it through the surge reservoir. The surge reservoir is a rectangular box which dampens the fluctuations in the flow produced by the pulsating action of the pump. This is important since it is assumed that the sand/water mixture enters the elbow in a steady flow.

The flow then reaches the top of a plexiglas tube which has a 1 inch internal diameter. The tube measures 6 feet in length and serves the purpose of being a type of flow straightener. Any swirling action or vortices induced in the pump or in the piping leading up to the plexiglas is reduced substantially by the time the flow reaches the outlet of this tubing. Therefore, the fluid enters the elbow essentially fully developed, steady, and vorticity free.

Attached at the bottom of the plexiglas tubing is a stainless steel compression fitting which holds the test elbow firmly in position. Part of the fitting is permanently attached to the tubing. The other half is held on to the elbow by means of two washers which fit securely around the outside diameter of the ell. The adjoining sections of the fitting, therefore, screw into one another, butting the elbow solidly up against the plexiglas tubing without having any frictional rubbing of the elbow during installation or removal. This is very important since precise weight measurements of the elbow are taken before and after each erosion test.

All erosion tests are made with one inch internal diameter copper elbows which are annealed at approximately 500 degrees F for

three hours prior to eroding. The majority of the runs use an elbow with an R/D value equal to 1.5, although a mitre bend with an R/D value of approximately 0.5, and an elbow with an R/D value of 5.0 are also tested as upper and lower bounds. The R/D value is defined as the ratio of the radius of curvature of the centerline streamline of the flow as it rounds the bend to the internal diameter of the pipe. In a mitre bend, the centerline streamline in a 1 inch I.D. pipe has an approximate radius of curvature of 0.5 inch.

In order to visually inspect the erosion profile obtained after a test, all elbows are sectioned and later held together by means of gasket material and a clamp (Figure 12). The internal wall of the outer section of each elbow is cleaned and polished before electroplating it with three successive layers of metal--silver, copper, and then silver again. These metals are chosen mainly because of their contrast in color and similarity in material properties. The electroplating process is outlined in detail in Appendix C.

By electroplating three layers of approximately equal thickness, it is easy to observe the progression of erosion penetration depth along the length of the elbow. When the first appearance of the copper metal base is sighted, the erosion test is stopped and that point is the point of maximum erosion. Typically, the tests last for about four hours, but often will exceed this time depending on how thick the layers of electroplated metal are and on the magni-

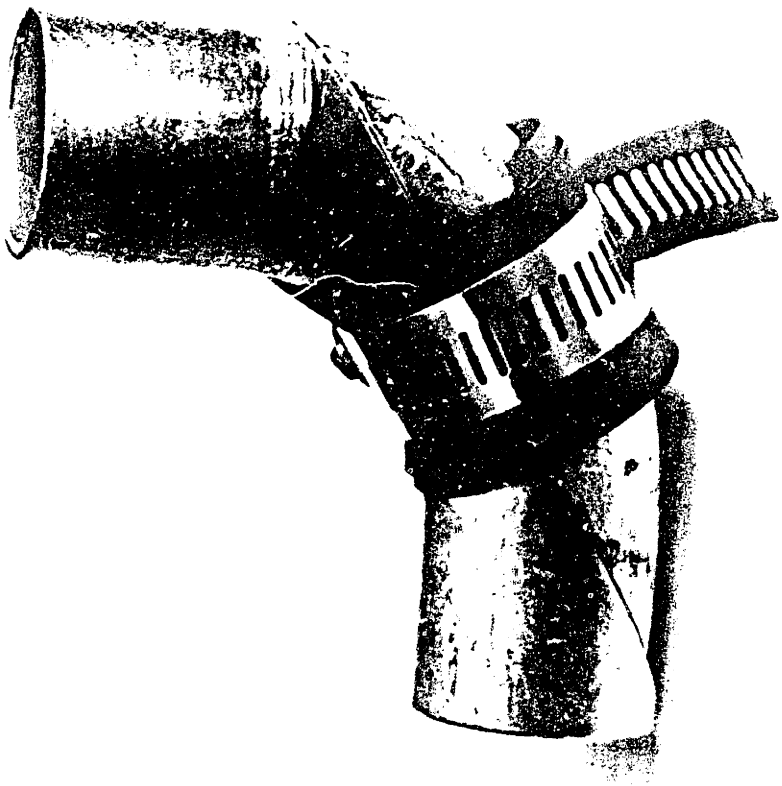

tude of the sand flowrate.

Although the pump has no speed or flowrate adjustment, water flowrate measurements are taken at the end of each run since the pump's routine performance is slightly variable depending on its working condition. Flowrate measurements are made by collecting water at the outlet of the plexiglas tube for a timed interval. The flowrate is calculated by dividing the volume of water accumulated by the collection time. The sand flowrate is measured in a similar manner except that a very fine sieve is used to collect the sand at the outlet of the tube. The sand is then left in the sieve to dry and when it is completely void of water, its weight measurement is recorded. The eroded elbow is weighed before and after each test using a chemical balance which measures accurately to the fifth decimal of a gram.

III. (2) Copper Elbow with An R/D Value Of 1.5

A total of nine experiments are performed using a 90 degree copper elbow which has an R/D value of 1.5. The radius of curvature is 1.5 inches and the internal diameter, 1 inch. The first four erosion tests use non-electroplated elbows, therefore no information regarding the point of maximum erosion is obtainable. However, for each, a wear coefficient, K_e, is calculated using the wear equation developed by E. Rabinowicz[5], as follows,

$$W_v = \frac{K_e M V^2 \beta}{g p_e} \tag{24}$$

where W_v is the volume of metal eroded, M, the total mass of impinging sand, V, the particle speed, and p_e, the penetration hardness. The β term is a function of the impingement angle which takes on the value 1.0 for angles between 10 and 60 degrees and 0.5 for angles between 0 and 10 degrees and between 60 and 90 degrees. This equation is very similar to that derived by Finnie except that its uncomplicated angle function makes it easier to apply.

In calculating the wear coefficient using this expression, a few changes are made. Namely, the velocity term in the expression is taken as that of the average fluid (mixture) velocity, not that of a single particle upon impact. This is done to allow one with no knowledge of the particle velocities to be able to make use of this equation. Also, since not all of the particles which pass through

the elbow impinge upon the wall, the value for the total mass of particles, M, is reduced by a factor of 2. The β value is 0.5 since the angle of impingement is always less than 10 degrees for the elbow. The results are presented in Table 2. The first four tests use 425 micron particles only.

In the next five runs that use this size elbow, the electroplating technique for visual observation of the erosion profile is employed. By knowing the thickness of each layer of electroplated metal, the erosion rate as well as the point of maximum erosion are ascertained. In an attempt to see the effect of particle size on the point of maximum erosion, particles measuring 95,270, 425, 605 and 1200 microns are tested. The final erosion specimens are photographed and are shown starting with Figure 13. The maximum wear point is the region where a solid copper area surrounded by a silver-copper-silver ring appears. In addition to a photograph, an exaggerated erosion profile of each specimen is drawn. Below each diagram is tabulated the erosion depth profile obtained at the end of the test.

The photographed erosion profile of the 425 micron sand particle test, shown in Figure 13, indicates a slightly unsymmetrical point of maximum erosion. However, the surrounding silver area is seen to be symmetrical. The exact location of the maximum wear point corresponds to the point where the silver area is eroded the greatest. In Figure 14, the maximum wear point, point 3, is located a little downstream of the projected area of the pipe. The angle measured

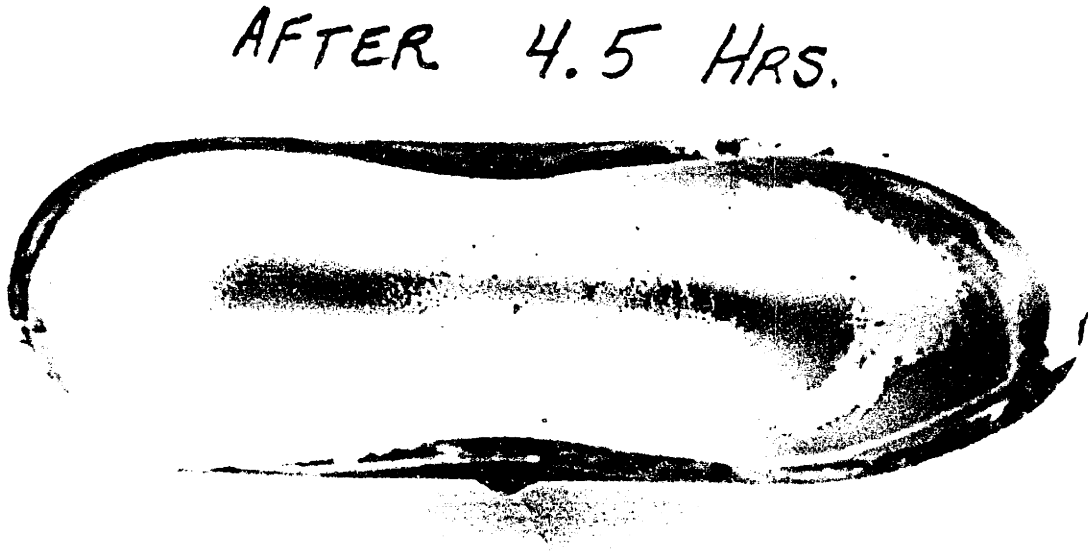

FIGURE 13 - EROSION SPECIMEN OF RUN #5--
425 MICRON SAND PARTICLES

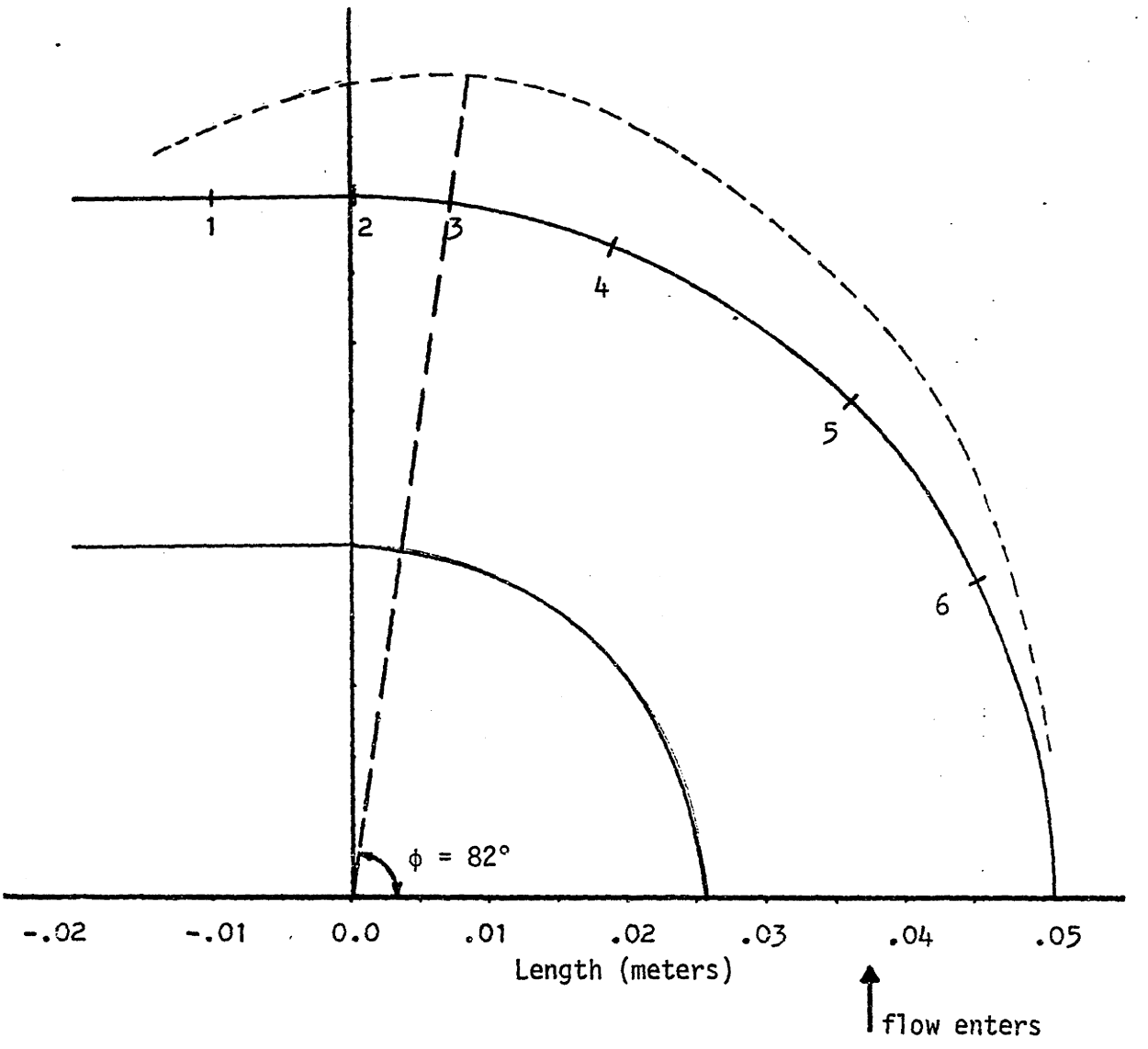

Depth of erosion after 4.5 hours (10^{-5} meters)

Point		
	1	2.31
	2	3.51
	3	3.95
	4	3.51
	5	2.31
	6	1.14

FIGURE 14 - EROSION DIAGRAM OF RUN #5

from the horizontal, ϕ, in the figure, which locates this point is approximately 82 degrees. Photographs of the elbow during different stages of erosion are given in Appendix D.

Run no. 6 is performed with 605 micron sand particles and a photograph of the resulting eroded elbow after 3.5 hours is shown in Figure 15. The point of maximum erosion occurs in almost the identical location as that of the previous case. However, another distinct point of erosion appears to the left of the main one. This spot is eroded due to a slight protrusion of the surface. The erosion profile sketch, shown in Figure 16, indicates that the point of maximum erosion occurs at an angle of 86 degrees from the horizontal.

For the next test, a substantially larger particle size is used -- 1200 microns. The particles are so large that they tear through the electroplated layers within a very short time. The final erosion specimen is photographed in Figure 17. Although a measure of the erosion rate is not obtainable, it is clear that the location of maximum erosion does not vary much from the two previous cases, if at all.

In run no. 8, 270 micron sand particles are chosen as the abrasives. A photograph of the electroplated elbow after six hours of erosion is shown in Figure 18. Again, the same location for the point of maximum erosion appears. The schematic diagram of the erosion profile, given in Figure 19, locates the point of maximum erosion at an angle, ϕ, of 82 degrees. A comparison photograph of eroded elbows, for the particle sizes of 270, 425, and 605 microns,

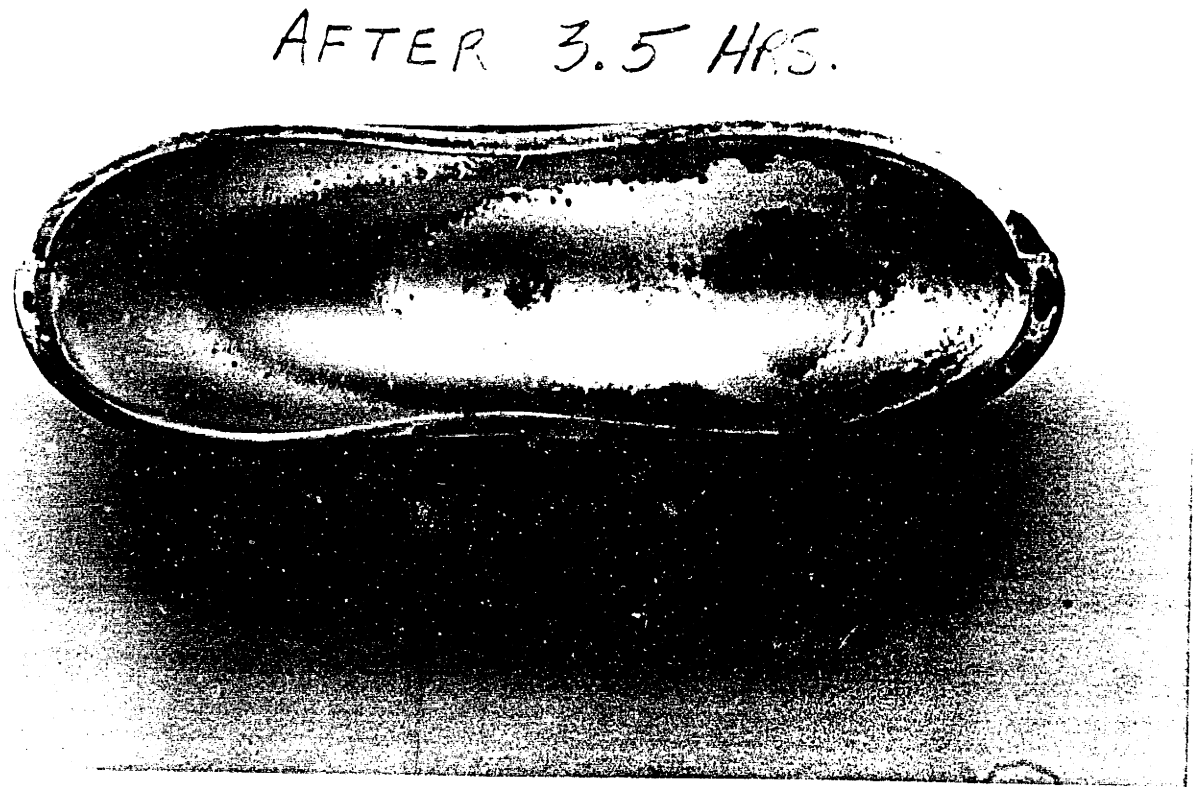

FIGURE 15 - EROSION SPECIMEN OF RUN #6 --
605 MICRON SAND PARTICLES

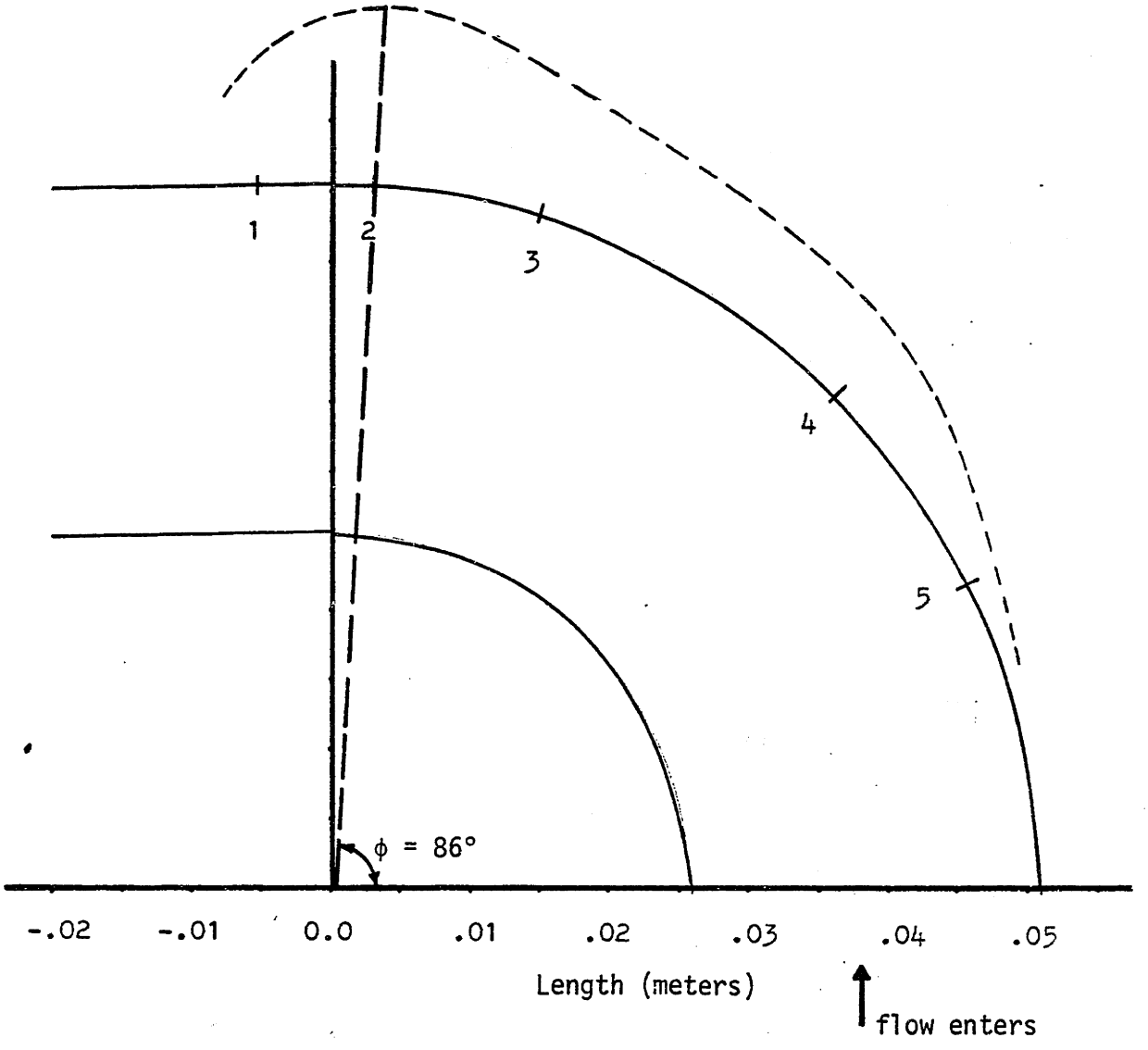

Depth of erosion after 3.5 hours (10^{-5} meters)

Point		
	1	3.84
	2	5.38
	3	3.84
	4	2.64
	5	.96

FIGURE 16 - EROSION DIAGRAM OF RUN #6

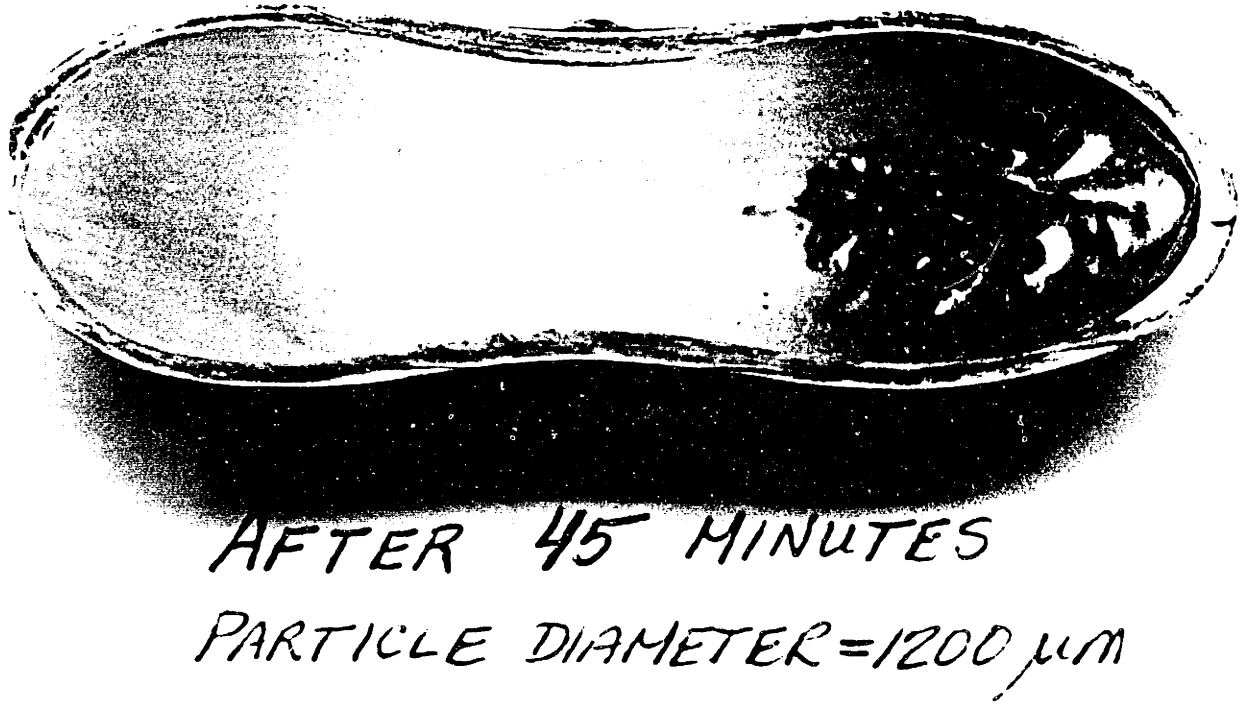

FIGURE 17 - EROSION SPECIMEN OF RUN #7 --
1200 MICRON SAND PARTICLES

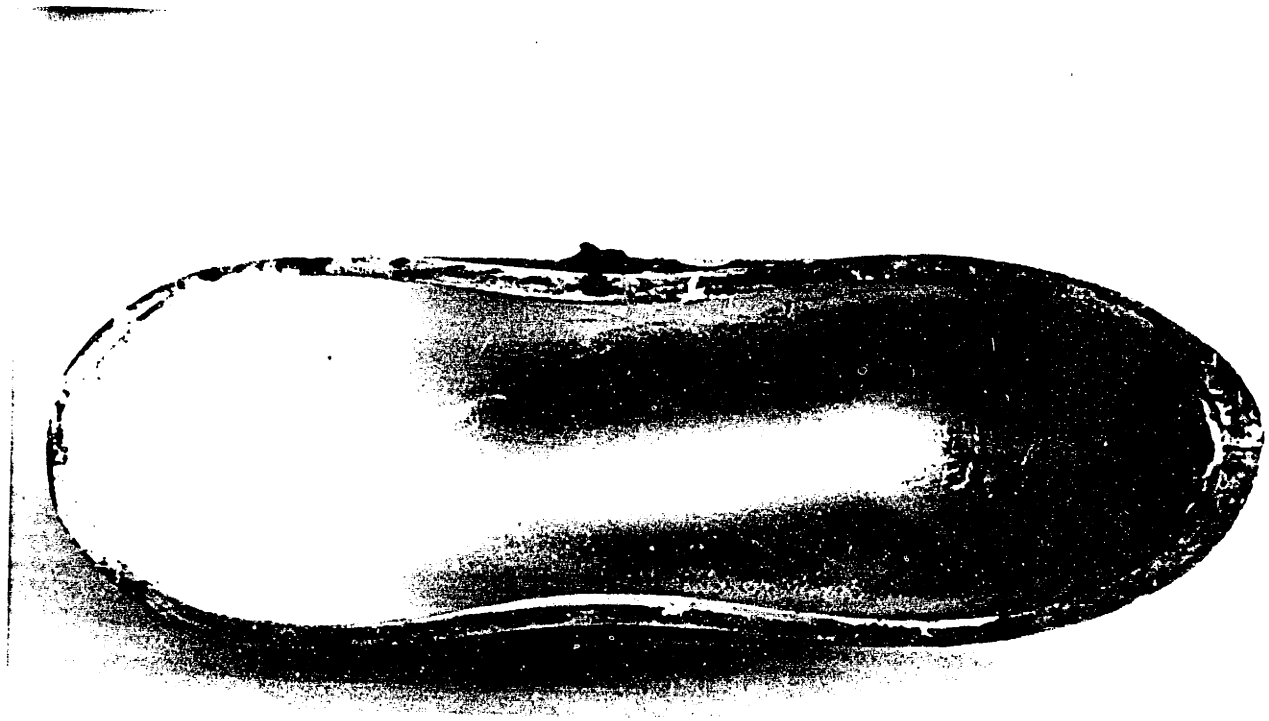

FIGURE 18 - EROSION SPECIMEN OF RUN #8 --
270 MICRON SAND PARTICLES

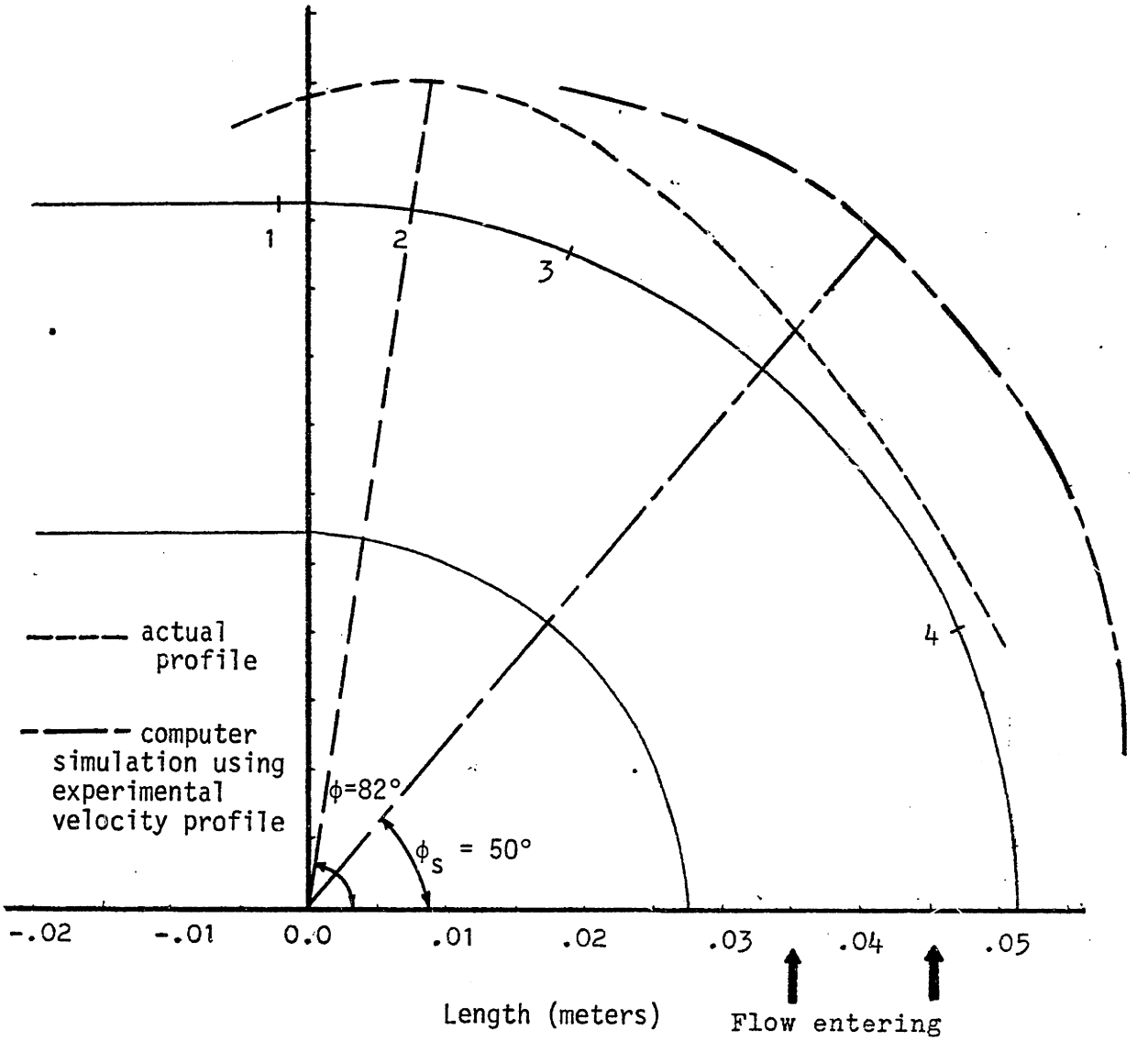

Depth of erosion after 6 hours (10^{-5} meter)

Point		
	1	2.94
	2	4.00
	3	2.94
	4	1.18

FIGURE 19 - EROSION DIAGRAM OF RUN #8 WITH A COMPARISON TO THE THEORETICAL PREDICTION

is shown in Figure 20. It is clear that the particle size plays a very weak role in determining the point of maximum erosion in an elbow of this size.

The previous chapter provides a theoretical model for the erosion process and uses 270 micron sand particles in a sample computer simulated prediction of the erosion profile. The experimental data of the simulation is taken directly from the data of run no. 8. In comparing Figures 8, 9 and 10 with the actual erosion profile, Figure 19, none of the three velocity fields of the model are seen to adequately predict the erosion profile. Of the three cases, the closest prediction to the actual result is the experimentally determined velocity profile case. This simulation predicts a maximum wear point at an angle, ϕ_s, of approximately 50 degrees. The difference in angle measurement between theory and experiment is 32 degrees. Simulations performed for the other size particles yield similar or higher values for the angle difference.

The final test which employs this particular size elbow, run no. 9, uses 95 micron silicon carbide particles. The silicon carbide is used instead of sand due to the unavailability of sand at this small particle size. Eventhough the properties of silicon carbide (SiC) are different from those of sand, namely a higher penetration hardness than sand, this does not effect the erosion process. As long as the abrasive is harder than the surface being eroded, then the degree of particle hardness is immaterial.

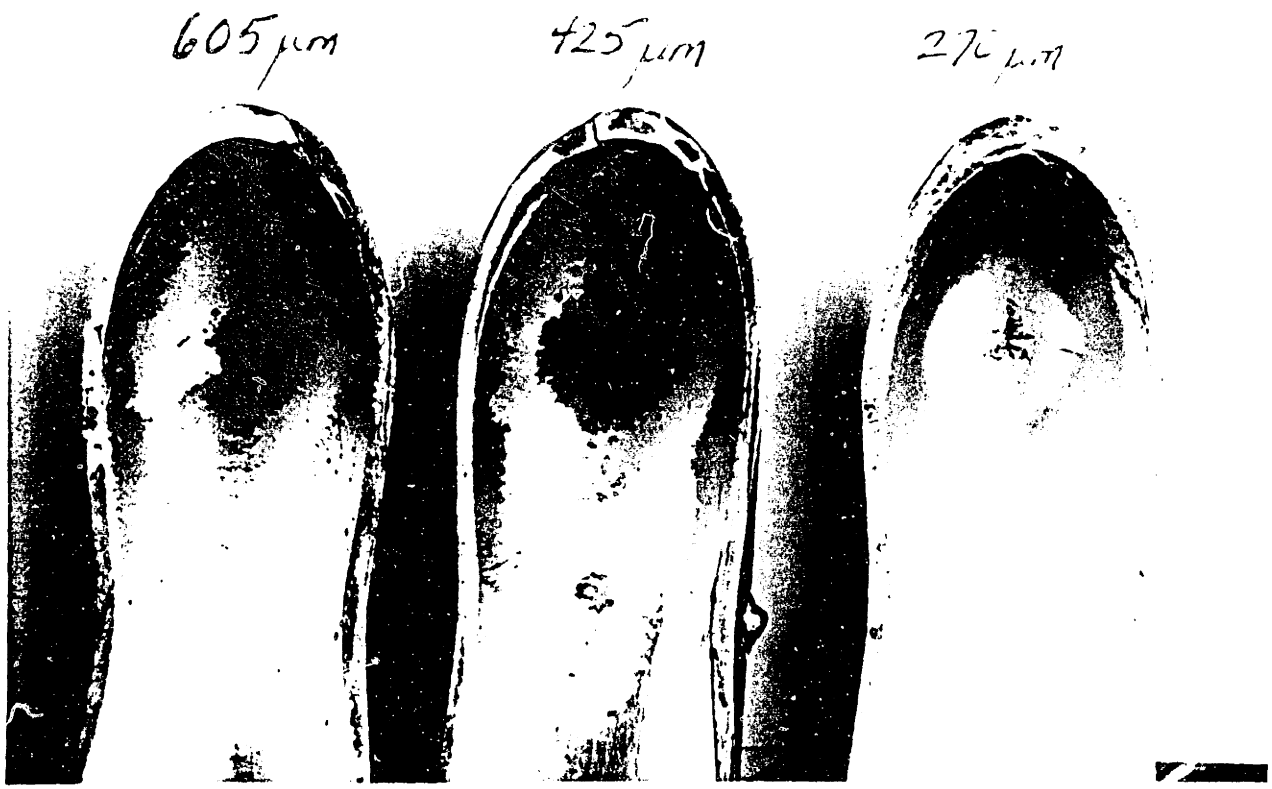

FIGURE 20 - COMPARISON PHOTOGRAPH OF EROSION SPECIMENS FROM RUNS #5, 6, and 8

The eroded elbow for run no. 9 is photographed in Figure 21. This profile appears different from the other erosion photos because the bottom electroplated silver layer is quite thin. However, upon close inspection, a thin silver band can be seen to surround the base copper metal at the point of maximum erosion. The erosion distribution diagram from this run, given in Figure 22, again locates the point of maximum erosion slightly downstream of the projected pipe area. The maximum erosion point location coincides with that obtained by other abrasive sizes. The angle made with the horizontal, ϕ, which locates the maximum wear point, is measured to be 89 degrees. The fact that this is slightly greater than the angle measured for the other particle sizes makes sense. The particles' inertia is so small that there is a tendency for them to follow the flow further downstream before striking the wall.

Examining Table 2, the wear coefficient for the nine runs is seen to vary within a narrow margin. The average value for K_e is 0.011.

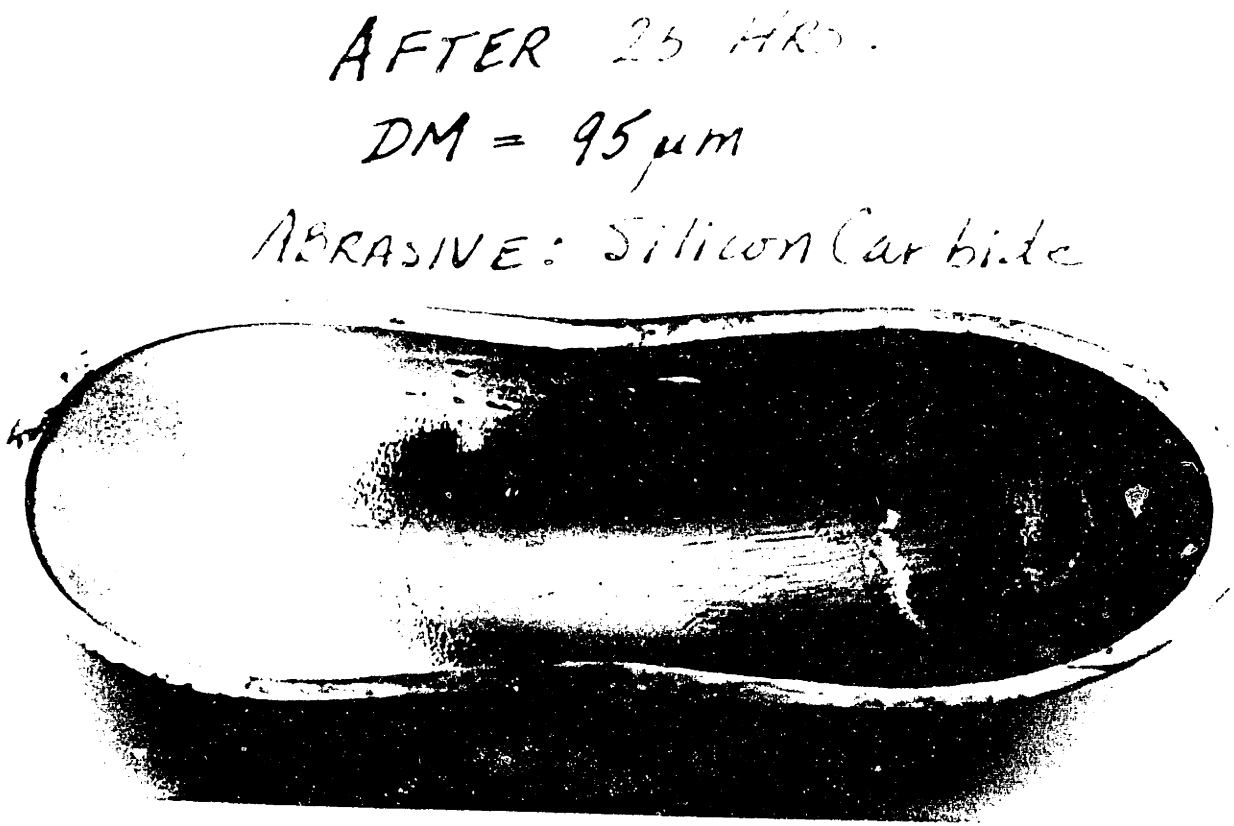

FIGURE 21 - EROSION SPECIMEN OF RUN #9 --
95 MICRON SILICON CARBIDE PARTICLES

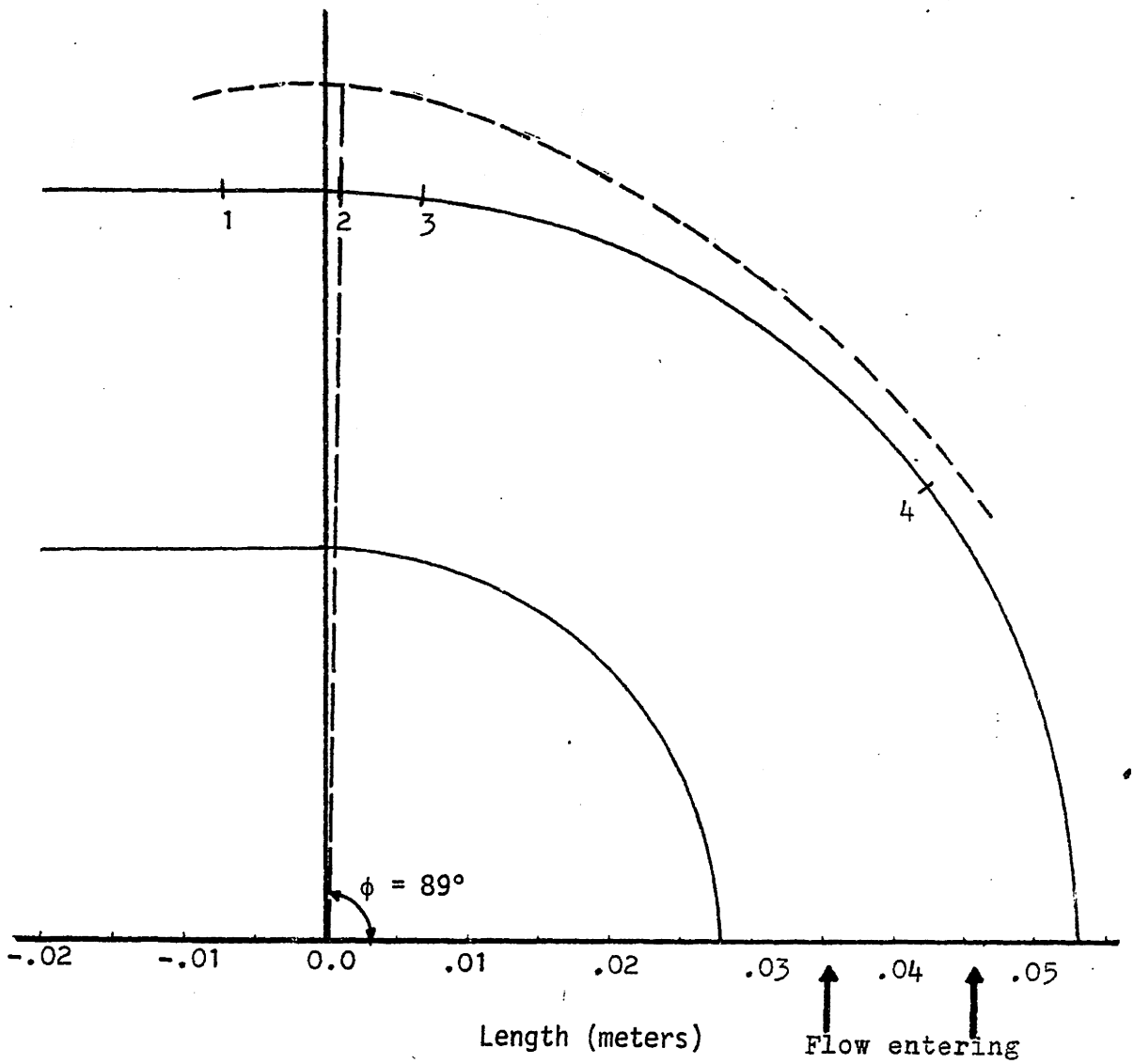

Depth of erosion after 26.7 hours (10^{-5} meter)

Point		
	1	2.88
	2	3.22
	3	2.88
	4	1.09

FIGURE 22 - EROSION DIAGRAM OF RUN #9

TABLE 2 - RESULTS OF EROSION TESTS WITH R/D = 1.5

Run #	Particle Size (μm)	Erosion Rate (g/hr)	Mass Ratio, γ (g part/g H_2O)	K_e
1	425	.0065	.0004	.021
2	425	.0691	.0086	.011
3	425	.0738	.0140	.007
4	425	.1131	.0203	.007
5 (electro.)	425	.1293	.0244	.011
6 (electro.)	605	.2359	.0389	.012
7 (electro.)	1200	no obtainable data		
8 (electro.)	270	.0745	.0164	.009
9 (electro.)	95	.0192	.0052	.007

III. (3) Copper Mitre Bend

In order to gain insight into the erosion of an elbow whose R/D value is a lower bound, the mitre bend is tested since the erosion behavior will be quite similar. Figure 23 shows a schematic drawing of a mitre bend where the radius of curvature, R, is approximately 0.5.

The mitre bend consists of two separate pieces of 1 inch I.D. copper pipe cut at 45 degree angles. The pieces are held together in a plexiglas fitting and then clamped. A photograph of the separate pieces of pipe positioned together without the fitting is shown in Figure 24.

The results of the erosion test, including the calculated wear coefficient, are listed in Table 3. The wear coefficient for the mitre bend exceeds the average wear coefficient for the previous size elbow by over a factor of 5. The lower section of the mitre bend is electroplated to enable one to detect the point of maximum erosion. In a photograph of the erosion profile, Figure 25, the maximum erosion point is located approximately 1.5 inches from the end. Besides this point, two other secondary points of erosion are located on the side and upper walls of this section. Figure 26 is a diagram of the erosion pattern as it would appear if the pipe were cut and flattened out. The secondary erosion points occur along the same circumference of the pipe. This would indicate a strong swirling or vortex action in the flow, commonly known as a secondary flow.

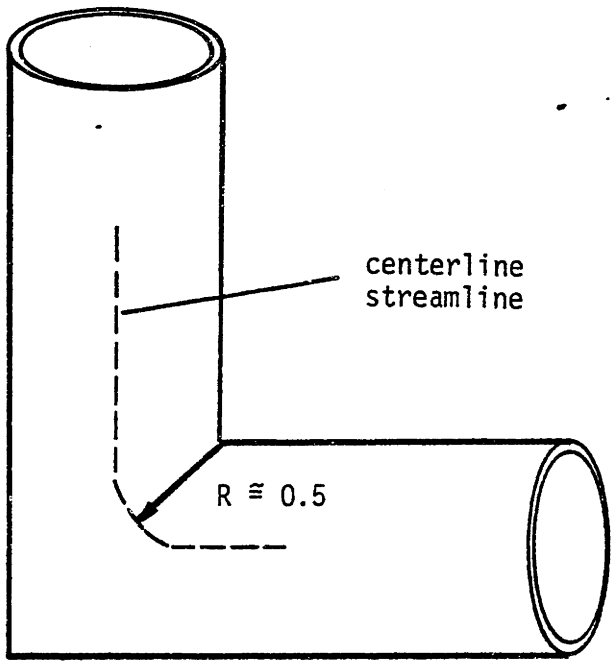

FIGURE 23 - SCHEMATIC DRAWING OF A MITRE BEND

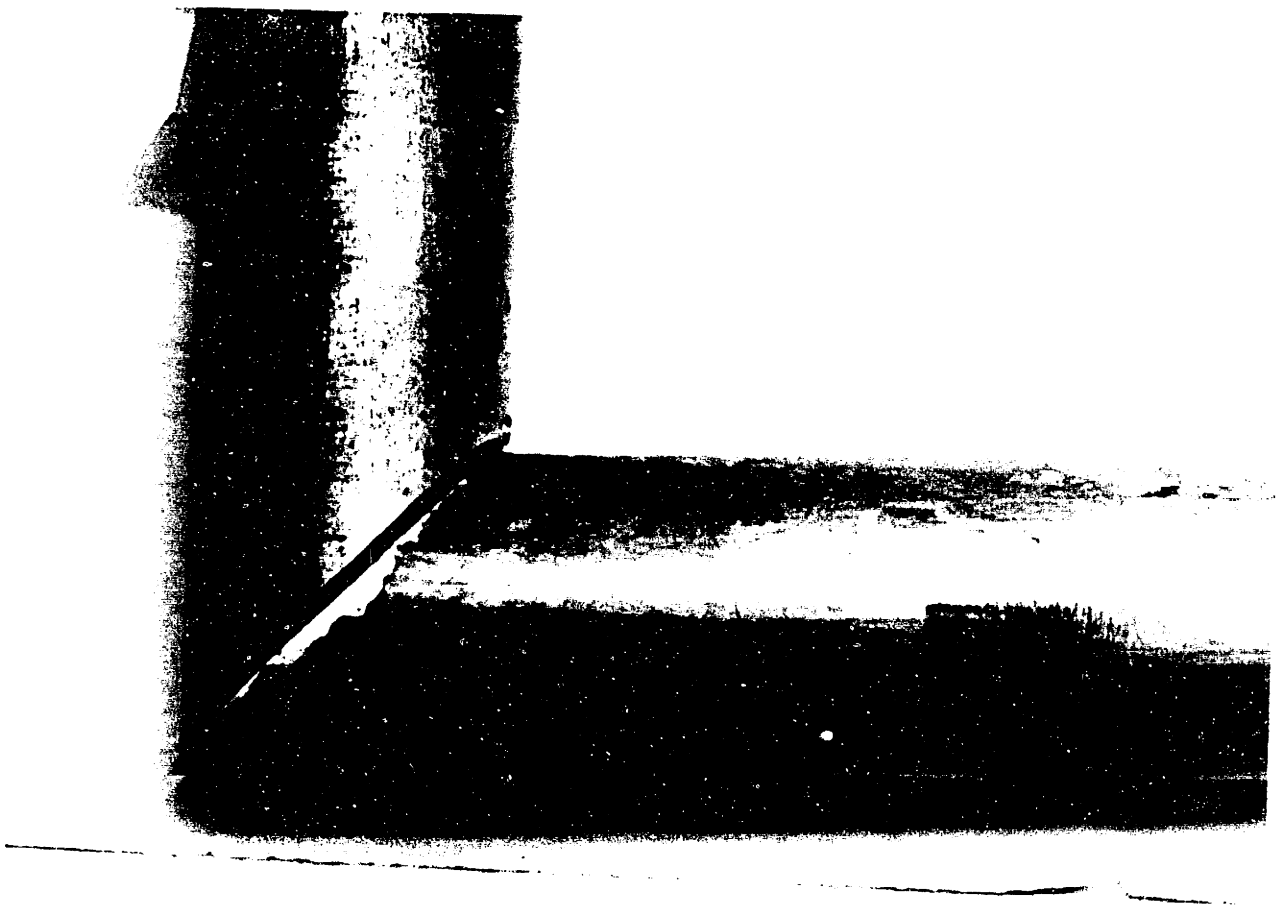

FIGURE 24 - MITRE BEND IN POSITION

TABLE 3 - DATA FOR RUN #10

Run no. 10	Mitre Bend
Particle Size	425 microns
Erosion Rate	0.3734 g/hr
Mass Ratio, γ	0.0121 g sand/g water
Erosion Time	3.25 hr
Wear Coefficient, K_e	0.057

FIGURE 25 - EROSION PHOTOGRAPH OF
MITRE BEND -- RUN #10

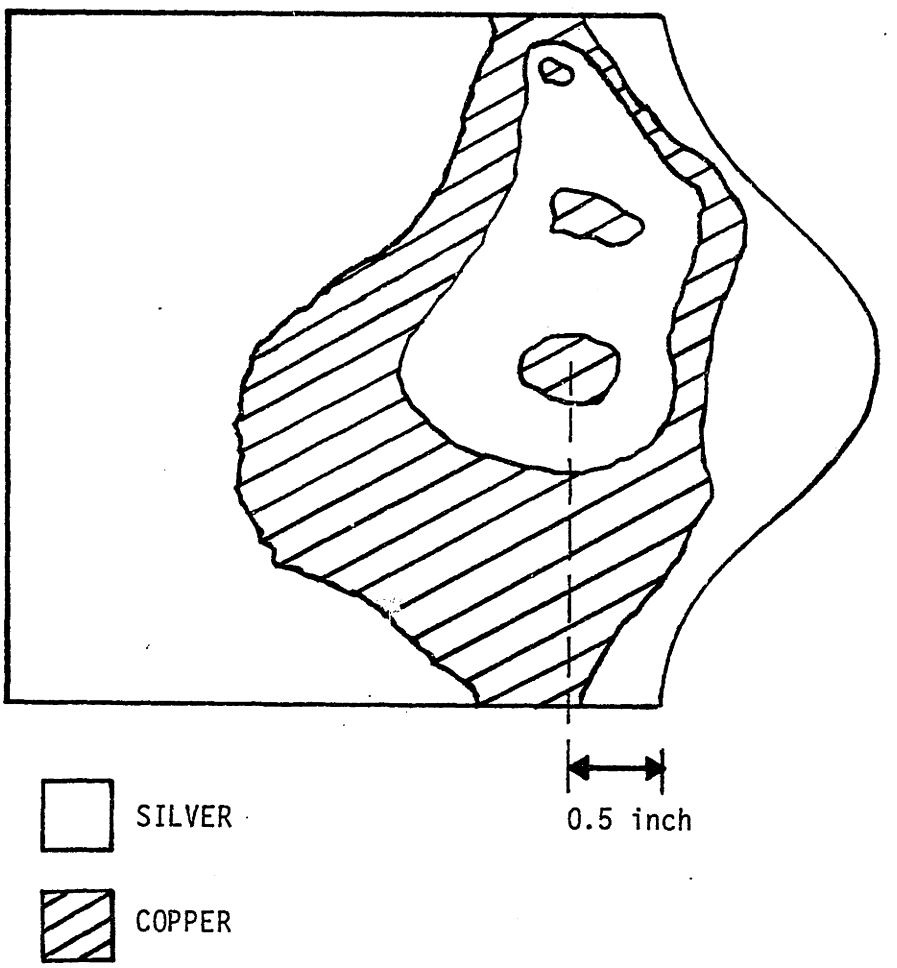

FIGURE 26 - MITRE BEND COMPLETE EROSION PATTERN

In Figure 27, the erosion profile along the main axis of the mitre bend is drawn. The maximum erosion point is located about .5 inch from the projected pipe area or at a measured angle, ϕ, of 105 degrees. In the elbow with R/D equal to 1.5, this distance is approximately 1 inch (measured along the horizontal axis).

The fact that the wear coefficient of the mitre bend is so much greater than that of the previously tested elbow, .057 compared to .011, may be attributed to several factors. In the wear coefficient calculation, the β value used, 0.5, corresponds to an angle of impact of less than 10 degrees. However, in the mitre bend, particles will most probably impact the wall at angles of between 10 and 60 degrees, which corresponds to a β value of 1.0. Also, in the case of the curved pipe, the total mass of sand striking the surface, M, is halved, under the assumption that only half of the particles entering the elbow will actually strike the wall. For the case of the mitre bend, it is reasonable to assume that all of the incoming particles will impact the wall. Therefore, these two changes in the calculation of the wear coefficient, reduces the K_e of a mitre bend by a factor of 4, or .014.

Furthermore, due to the dissimilarity in geometry, the mitre bend may exhibit a different frequency and effect of secondary impingements. This would also result in a different value for K_e.

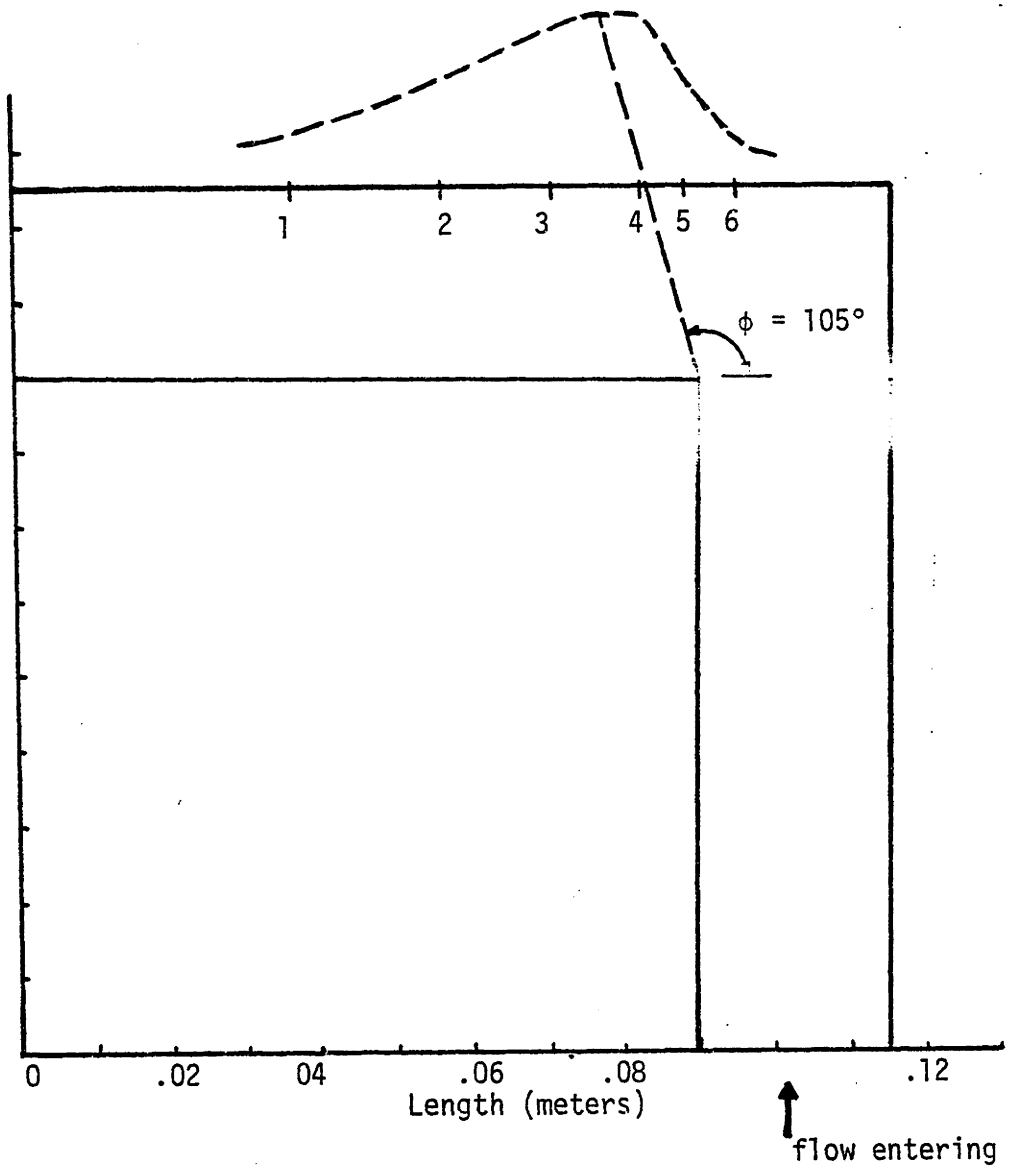

Depth of Erosion after 3.25 hours (10^{-5} meter)

Point		
	1	1.6
	2	3.1
	3	4.6
	4	4.6
	5	3.1
	6	1.6

FIGURE 27 - MITRE BEND MAIN AXIS EROSION PROFILE

III. (4) Copper Elbow with An R.D Value Of 5.0

An elbow with an R/D value of 5.0 is tested to see how the erosion pattern differs for a bend with a more gradual curvature. Although this does not represent the limiting case, in commercial use, seldom does a 90 degree elbow have a larger ratio of turning radius to internal diameter.

In view of the large size of this elbow, only a portion of the outer wall section is electroplated. Figure 28 is a photograph of the elbow with the electroplated section alongside. The erosion profile is shown by itself in the photograph of Figure 29. The erosion test is stopped soon after the first sign of the base metal appears. This insures locating the point of maximum erosion accurately.

An obvious difference between the wear pattern of this elbow and that of the previous elbows, is the broader extent of the erosion. For the first elbow, the erosion is spread over a narrower length of pipe. For the mitre bend, the erosion effects are even more localized. Table 4 lists the pertinent data for run no. 11. The wear coefficient, K_e, is half that of the mitre bend erosion test.

Figure 30 is the erosion distribution diagram obtained after 11.25 hours. The angle, ϕ, which locates the point of maximum erosion, is measured to be 75 degrees. The average value of ϕ for the electroplated elbows with R/D equal to 1.5, is 85 degrees. Taking into consideration the disparity in elbow size, this is not a large difference. The point of maximum erosion is located approximately 3 inches down-

stream of the projected pipe area, where the distance is measured along the horizontal axis. This compares to .5 inch for the mitre bend and 1 inch for elbow with R/D equal to 1.5.

FIGURE 28 - EROSION SPECIMEN OF RUN #11
WITH THE ELBOW OF R/D = 5.0

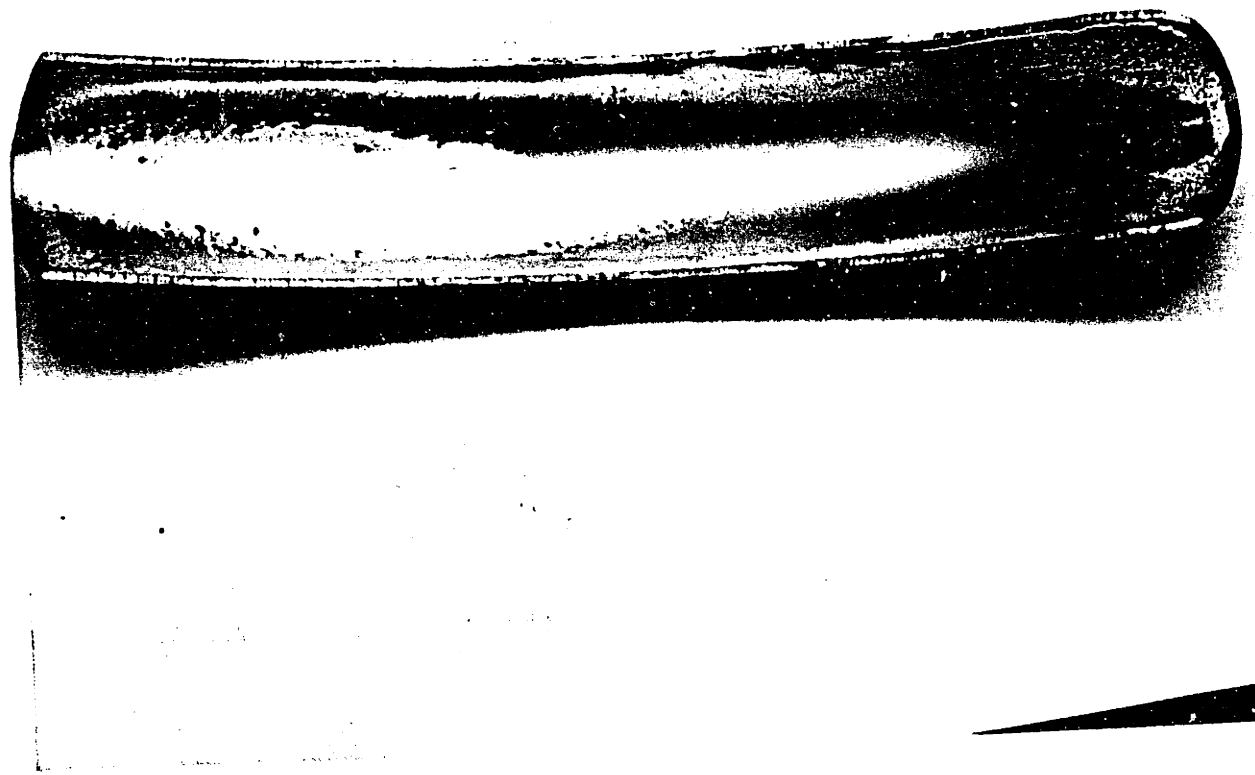

FIGURE 29 - EROSION SPECIMEN OF RUN #11 --
425 MICRON SAND PARTICLES (R/D = 5.0)

TABLE 4 - DATA FOR RUN #11

Run no. 11	R/D = 5.0, I.D. = 1 inch
Particle Size	425 microns
Erosion Rate	0.1198 g/hr
Mass Ratio, γ	0.0080 g sand/g water
Erosion Time	11.25 hr
Wear Coefficient, K_e	0.028

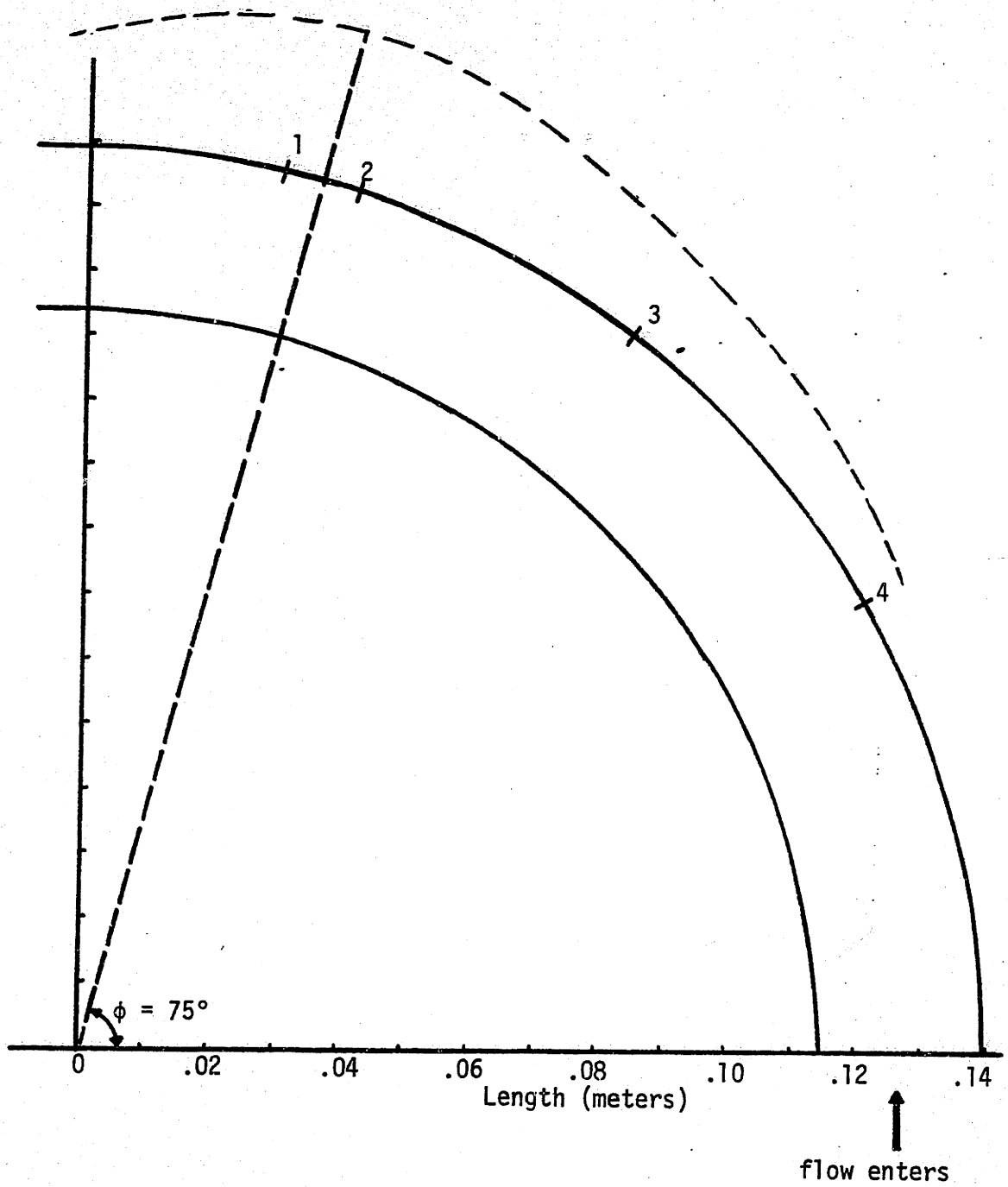

Depth of erosion after 11.25 hours (10^{-5} meter)

Point		
	1	4.8
	2	4.8
	3	3.3
	4	1.5

FIGURE 30 - EROSION DIAGRAM OF RUN #11

IV. DISCUSSION OF RESULTS

The most prominent observation one makes from this report is the rather unexpected consistency in the location of maximum wear point for an elbow whose R/D value is 1.5. The fact that in testing several abrasive sizes, which vary by over an order of magnitude, the maximum wear point varies very little, indicates that strong, secondary flow effects are present. These unaccounted flows, which cannot be modeled in a two-dimensional analysis, probably are to blame for the inaccurate erosion predictions of the theoretical model. While the presence of secondary flows in a pipe elbow is not unexpected, their effect on the particle trajectories is much stronger than was originally anticipated.

When a fluid flows through a curved pipe, a pressure gradient across the pipe is required to balance the centrifugal force arising from the curvature. The pressure at the larger radii of the bend is greater than that at the smaller radii. As an outcome, a flow is set up which is directed outwards in the center and inwards (i.e., towards the center of curvature) near the wall, Figure 31. This is the secondary flow. As a result of this flow, the region of maximum velocity in the main stream is shifted toward the outer part of the wall. This would corroborate the measured velocity profile of Figure 4.

As the R/D values of elbows decrease, the strength of the secondary flows increase. It has already been shown how the helical

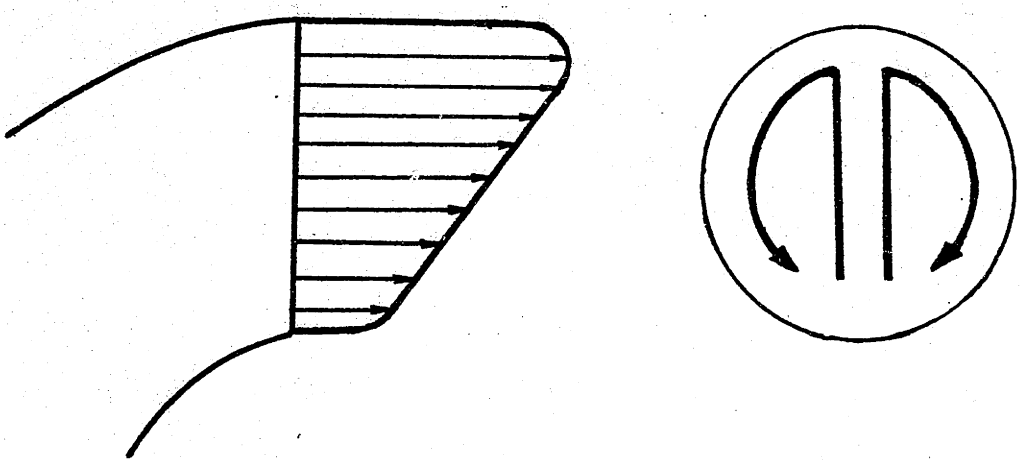

FIGURE 31 - SECONDARY FLOWS

action of the flow in a mitre bend (R/D approx. equal to 0.5) causes a 360 degree erosion pattern (Figure 26). It is believed that this type of flow behavior is responsible for propelling a majority of the particles at the same focused point along the elbow wall. For the R/D value of 1.5, the average angle, ϕ, for the location of maximum wear, is measured to be 85 degrees. This point corresponds to a distance of 1 inch downstream of the projected pipe area, as measured along the horizontal axis. For the elbow whose R/D value is 5.0, these measurements are 75 degrees and 3 inches downstream of the projected pipe area, respectively. The mitre bend, which represents the most concentrated wear profile, experiences a maximum wear point only .5 inch downstream of the pipe area projection at an angle, ϕ, of 105 degrees.

In view of the fact that the theoretical model of erosion for an elbow is not very accurate, and that its application is rather long and complex, a simpler, approximate technique is needed which would render a rough, conservative prediction of wear. Using the wear coefficient found for the mitre bend, namely .057, an upper bound for wear can be calculated with the use of Eqn. 24. The β value used should be 0.5 and the sand flowrate should be divided by 2 to account for non-impinging particles. The velocity used is the mixture velocity. If the volume of wear found by this calculation is divided by the pipe cross-sectional area, a conservative prediction of the erosion depth is obtained. This is summarized below.

$$\text{Erosion depth, } h_m = \frac{W_v}{A} = \frac{K_e\, M\, V^2\, \beta/g\, p_e}{\pi\, D^2/4} \qquad (25)$$

where, $K_e = 0.057$

$\beta = 0.5$

M = 1/2 (actual sand mass)

Specifically, for run no. 5,

V = 5.0 m/s

$p_e = 107.5 \times 10^6$ kg/m^2

D = .0254 m (1 inch)

M = 1/2 (836.4 kg) = 418.2 kg

Substituting these values, the conservative estimate of erosion depth, h_m, is 55.8×10^{-5} meter. Table 5 lists the actual erosion depths obtained at the point of maximum erosion. Also tabulated are the predictions of erosion depth using the aforementioned technique. It is seen that the predicted erosion depths exceed the actual depths by over an order of magnitude. The location of maximum wear can be assumed to be at an angle, ϕ, of 85 degrees for R/D equal to 1.5, and 75 degrees for R/D equal to 5.0. Values of R/D in between these can be interpolated to find ϕ.

The technique outlined above allows for a conservative prediction of erosion depth in a 1 inch I.D., 90 degree elbow. Further work, using different pipe sizes, is needed before predictions covering all possible elbow configurations may be made.

TABLE 5 - CONSERVATIVE PREDICTION OF EROSION DEPTH FOR 1 INCH I.D. ELBOWS

Run #	R/D value	Actual Erosion Depth at Point of Maximum Erosion (10^{-5} m)	Predicted Erosion Depth at Point of Maximum Erosion (10^{-5} m)
5	1.5	3.95	55.8
6	1.5	5.38	55.5
8	1.5	4.00	56.2
9	1.5	3.22	69.5
11	5.0	4.80	55.9

V. CONCLUSIONS AND RECOMMENDATIONS

The average wear coefficient for an elbow whose R/D value is 1.5 is determined to be .011. The effect of particle size on the location of the maximum erosion point is found to be negligible in this size elbow. Secondary flow effects are believed to produce the consistency in the location for the maximum erosion point, namely an angle, ϕ, equal to 85 degrees.

The mitre bend erosion test substantiates the strong effect of secondary flows on the erosion profile. A wear coefficient, K_e, of .057 is calculated.

A more gradual bend curvature, an R/D value of 5.0, is tested and results yield a wear coefficient of .028. The maximum erosion point occurs at an angle, ϕ, of 75 degrees. The distance between this point and the projected pipe area is measured to be 3 inches. This distance decreases with the R/D value of the elbow; for the R/D value of 1.5, this measurement is 1 inch and for the mitre bend, 0.5 inch.

A two-dimensional, theoretical model which tracks the particle trajectories and then calculates the wear at impingement, does not accurately predict the erosion profile of an elbow. A simple, conservative technique is outlined to predict the location and magnitude of the maximum erosion depth of a 1 inch I.D., 90 degree elbow. Further tests, on different pipe sizes, is needed before a completed wear prediction technique, which covers many geometries, is obtained.

NOMENCLATURE

A	cross-sectional area of pipe
A_p	frontal area of particle in streamwise direction
b	half width of two-dimensional elbow channel
C	constant
C_d	drag coefficient
d	particle diameter
D	pipe diameter
g	gravity
h_m	depth of erosion
H	height of two-dimensional elbow channel
k	constant
K	constant
K_e	wear coefficient
m	single particle mass
M	total particle mass which impinged upon surface
n	normal direction
Np	total number of particles entering elbow per unit time
p	pressure
p_e	penetration hardness
Q	volumetric flowrate
r	radial direction measured from center of curvature of elbow centerline

NOMENCLATURE (Cont.)

R	radius of curvature of centerline streamline of elbow
Re	Reynolds number
R_o	radius of curvature of outer wall of elbow
S	position along the curved outer wall of elbow
u	x direction component of fluid velocity
v	y direction component of fluid velocity
V	particle velocity
V_e	mixture velocity entering elbow
V_s	fluid streamline velocity
W	mass of metal eroded
W*	dimensionless mass of eroded metal
W_v	volume of metal eroded
$\dot{x}$	x component of particle velocity
$\dot{y}$	y component of particle velocity

Greek Symbols

α	angle of impact
β	angle function in wear equation
ε	correction factor to wear equation
γ	mass ratio of sand to water
ρ_f	density of liquid
ρ_p	particle density

Greek Symbols (Cont.)

ρ_s	metal density
ϕ	angle location of actual maximum point of erosion
ϕ_s	angle location of theoretical maximum point of erosion
ν	kinematic viscosity

REFERENCES

1) Finnie, I., "The Mechanism of Erosion of Ductile Metals", Proc. 3rd U.S. Natl. Congress Appl. Mech., 1958, pp. 527-532.

2) White, F. M., Viscous Fluid Flow, McGraw-Hill, Inc., New York, 1974, p. 209.

3) Finnie, I., "The Mechanism of Erosion of Ductile Metals", Proc. 3rd U.S. Natl. Congress Appl. Mech., 1958, pp. 527-532.

4) Benchaita, M., "Erosion of Metal Pipe by Solid Particles Entrained in a Liquid", Dept. of Mechanical Engineering, M.I.T., 1979.

5) Rabinowicz, E., "The Wear Equation for Erosion of Metals by Abrasive Particles", Dept. of Mechanical Engineering, M.I.T., 1979.

6) Pao, Richard H., Fluid Dynamics, Merrill Books, Inc., Columbus, 1967.

7) Lowenheim, F. A., Modern Electroplating, John Wiley & Sons, Inc., New York, 1974.

APPENDIX A - Hyperbolic Velocity Profile Derivation[6]

The two-dimensional velocity profile derived using the Euler-n equation is developed by considering the closed conduit to be rectangular in cross section. The centroidal axis of the conduit contains a circular bend with radius R as shown in Figure 2. It is assumed that the incompressible flow in the conduit is steady and frictionless, and that the streamlines of the flow in the bend are also circular arcs with centers on the axis of the bend. Consider a streamline with radius r. The equation of motion for any fluid particle on this streamline is Euler's equation since the flow is incompressible and frictionless. Using streamline coordinates, the normal component of Euler's equation for a steady, incompressible flow is written as,

$$- \frac{1}{\rho_f} \frac{\partial p}{\partial n} - g \frac{\partial z}{\partial n} = \frac{V_s^2}{r} \tag{26}$$

where $-\partial z/\partial n$ represents the cosine of the angle between the n-axis and the negative z-axis, which has been chosen as the direction of gravity. It should be pointed out that the n-axis is taken in a direction toward the center of curvature of a curved streamline. Hence dn = -dr, and the above equation becomes,

$$\frac{\partial}{\partial r} \left(\frac{P}{\rho_f} + gz\right) = \frac{V_s^2}{r} \tag{27}$$

Furthermore, Bernoulli's equation,

$$\frac{P}{\rho_f} + gz + \frac{V_s^2}{2} = \text{constant} \tag{28}$$

may also be applied to any streamline in this flow. Partial differentiation of Bernoulli's equation with respect to r yields

$$\frac{\partial}{\partial r}\left(\frac{P}{\rho_f} + gz\right) + V_s \frac{\partial V_s}{\partial r} = 0 \tag{29}$$

By substituting equation (29) into equation (27), gives

$$\frac{V_s^2}{r} + V_s \frac{\partial V_s}{\partial r} = 0 \tag{30}$$

Then separation of variables yields,

$$\frac{\partial r}{r} + \frac{\partial V_s}{V_s} = 0 \tag{31}$$

This differential equation is readily integrated to give

$$\ln r + \ln V_s = \ln (rV_s) = \text{constant} \tag{32}$$

Therefore,

$$r V_s = K \quad \text{or} \quad V_s = \frac{K}{r} \tag{33}$$

where K is a constant of integration. This equation shows that the maximum and minimum velocities occur at the inner and outer radii of the bend, respectively. The velocity profile represented by Eq. (33) is evidently an arc of a hyperbola as shown in the figure.

The constant K is determined by using the continuity equation:

$$Q = \iint_A V_s \, dA = K \iint_A \frac{dA}{r} \tag{34}$$

Hence

$$K = \frac{Q}{\iint_A (dA/r)} = \frac{Q}{H \int_{R-b}^{R+b} (dr/r)} \tag{35}$$

$$K = \frac{Q}{H \ln((R+b)/(R-b))} \tag{36}$$

This velocity profile was used because at the time, it was felt that it adequately described the velocity field in an elbow without resorting to a three-dimensional analysis.

APPENDIX B - Correction Factor to Finnie's Wear Equation

An inspection of Figure 5, Finnie's predicted and corrected relative weight loss curve, reveals that Finnie's model predicts an accurate weight loss for angles less than 17 degrees. Finnie suggests adding an amount δ to the weight loss at 90 degrees which is the average for all angles between 17 degrees and 90 degrees. The Finnie equation is as follows,

$$W = \frac{\rho_s m V^2}{2p_e 2g} F(\alpha) \tag{37}$$

The dimensionless wear equation would be written as,

$$W^* = \frac{W p_e g}{\rho_s m V^2} = \frac{F(\alpha)}{4} \tag{38}$$

$$\text{where } F(\alpha) = \sin 2\alpha - 3\sin^2\alpha \qquad \alpha \leq 18.5^\circ$$

$$F(\alpha) = \frac{\cos^2\alpha}{3} \qquad \alpha > 18.5^\circ \tag{39}$$

If the sum of $F(\alpha)/4$, evaluated for all angles between 17 and 90 degrees, is divided by the total number of angles evaluated, the average dimensionless wear for these angles, δ, is determined. For angles between 17 and 90 degrees, a proportional amount, ε, in Figure 5, is added to the weight loss curve. Therefore, this correction factor is

written as,

$$\varepsilon = \frac{\delta}{73}\ (\alpha - 17°) \qquad \alpha \geq 17°$$
$$\varepsilon = 0 \qquad \alpha < 17° \tag{40}$$

where $\delta = .130$.

APPENDIX C - Electroplating Process Used in Plating Copper Elbows

The electroplating process is not a very complicated operation; however, some guidelines should be mentioned if it is desired to repeat this procedure. The first and most important step in electroplating is the cleaning and/or etching of the surface to be plated. Some authorities on the subject believe that electrocleaning with a prepared solution is the best means to accomplish this. The reason for having such a clean surface is to avoid any peeling or chipping which results when a close bond does not develop between the base metal surface and the electroplated metal layers.

In this experiment, the copper elbow to be plated is sawed obliquely into two sections. The outer section contains the wall which experiences the most erosion. It is the internal surface of this section which is plated.

The surface is prepared for electroplating by first polishing with a fine emery cloth or steel wool. This removes the heavy dirt and rust and also smoothes out any surface imperfections. The elbow is then etched using approximately a 30% solution of nitric acid and water. A few minutes of soaking in this bath followed by a thorough rinsing using distilled water should be sufficient.

The next step is preparing the electrodes. Copper wire (1/8 inch) about 8 inches in length is soldered to a point on the outside area of the elbow. A butane torch is needed to provide enough heat to melt the solder on the pipe. After the wire is

firmly attached and the solder is allowed to cool, an electrically insulating varnish called Microstop is painted on the outside area. This insulator is applied wherever electroplating is not needed. The soldered area is completely covered with this substance since the introduction of foreign metallic ions from the solder could contaminate the plating solution. The edges which are produced when the elbow is cut are also covered with Microstop since rough edges will plate out preferentially and produce an uneven coating.

A strip of silver which is 3 inches in length, 0.5 inch in width, and .020 inch thick, is used as the silver anode. The particular size and shape was dictated by the geometry of the cathode (the elbow). The projected length of the area to be plated on the elbow is approximately 3 inches and its width is about 1 inch. For copper plating, a similarly sized piece of copper sheet is used. The metal strip is soldered to copper wire and then Microstop is applied as before. The anode is given a slight curvature so as to conform nicely to the shape of the cathode. Ideally, all points on the cathode are to be equidistant from corresponding points on the anode to avoid having preferential plating areas.

The next step is the preparation of the plating solutions. Both copper and silver plating solutions are cyanide solutions and caution is needed in handling the chemicals. The compositions and operating conditions for the silver and copper plating baths are listed below[7]. The chemicals are mixed in distilled water and periodic filtration is required to remove harmful impurities.

Silver Cyanide Plating Solution:

Silver cyanide	45-50 g/l
Potassium cyanide	45-50 g/l
Potassium hydroxide	10-14 g/l
Potassium carbonate	45-80 g/l
Potassium nitrate	40-60 g/l

Operating conditions:

Temperature	20-28°C
Current density	0.5-1.5 A/dm^2 (with agitation)
Cathode efficiency	100%
Anode efficiency	100%
Ratio of anode to cathode area	not less than 1:1

Copper Cyanide (Strike) Solution:

Copper cyanide	15 g/l
Sodium cyanide	23 g/l
Sodium carbonate	15 g/l

Operating conditions:

Temperature	41-60°C
Cathode current density	1.0-3.2 A/dm^2
Anode current density	0.5-1.0 A/dm^2
Cathode efficiency	10-60%
Ratio of anode to cathode area	3:1

It should be noted that although the rules for anode and cathode current densities and area ratios are listed, they cannot always be strictly abided by. In practice, geometric and/or other constraints make it difficult to follow these guidelines at all times. Eventhough satisfactory results are obtained, better plating jobs may result when all the recommended conditions are met. One possible side effect of a grossly inaccurate area ratio in the copper plating process

is the blackening of the copper anode. Although this does not seem too detrimental to the process, the anode should be cleaned as often as possible.

A schematic diagram of the electrical components and connections involved in the plating operation is shown in Figure 32. The pyrex container of plating solution rests on a combination hot plate/stirrer. A rotating disk under the plate surface drives a magnetic bar which is placed in the solution. This induced spinning motion of the bar agitates the mixture. The anode is connected to an ammeter which monitors the current flowing through the circuit. The ammeter connects to the positive terminal of a d.c. power supply. The cathode connects to the negative terminal. The electrodes are positioned close enough to each other so that they are at all points equidistant, but not close enough to make contact. Also, the electrodes are fully immersed in the plating solution.

The amount of metal which is plated onto the elbow is predetermined using electrolytic chemistry. A sample calculational sequence is given below for silver electroplating:

Area to be plated, A_s: 40 cm^2

Depth of layer required, Δd: .0015 cm

Volume of silver, $A_s \Delta d$: .06 cm^3

Density of silver: 10.49 g/cm^3

Mass of silver required, M_s: .6294 g

Current density (cathode): 1.0 A/dm^2

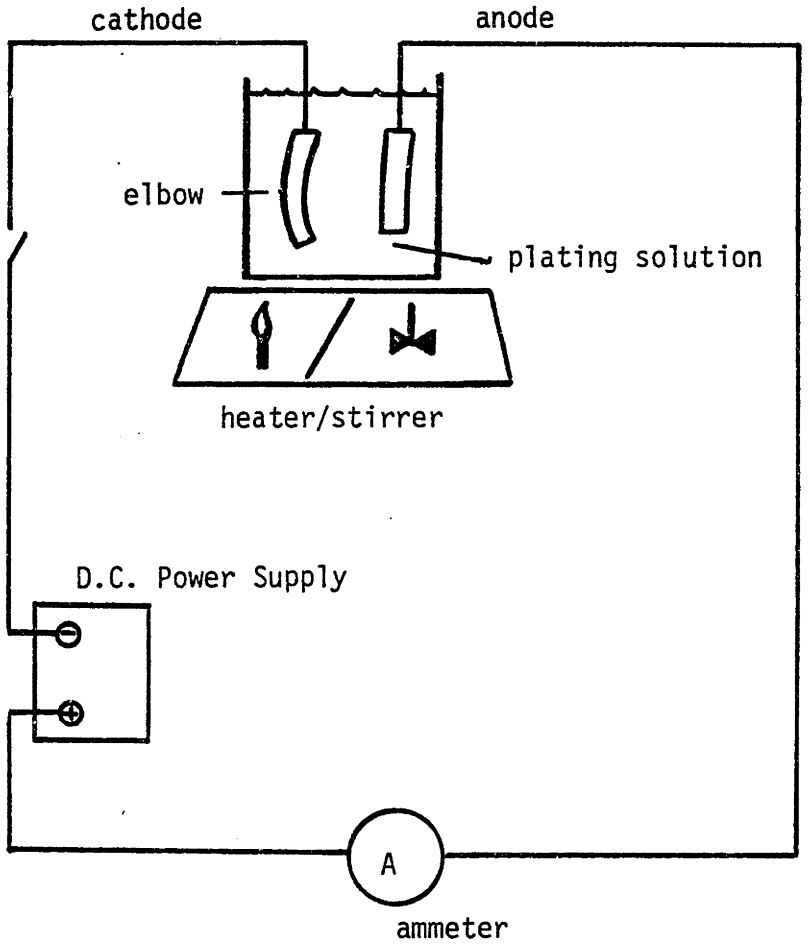

FIGURE 32 - SCHEMATIC OF ELECTROPLATING CIRCUIT

Current: $i = (1.0\ A/dm^2)(40\ cm^2)(1\ dm^2/100\ cm^2)$

$i = 0.4\ A$

Charge transmitted in time t: .4t coulombs

Plating efficiency: 100%

Mass transferred in time t:

$$M_s = \left(\frac{.4t\ \text{coulombs}}{96490\ \text{coulombs/Faraday}}\right)\left(\frac{1\ \text{gram-equiv.}}{1\ \text{Faraday}}\right)\left(\frac{107.868\ \text{grams Ag}}{1\ \text{gram-equiv.}}\right)$$

$$\times\ (100\%\ \text{efficiency})$$

Equating the mass of silver required to this expression gives the plating time, t, in seconds, necessary to transfer 0.6294 grams of silver from anode to cathode. For this case it takes 23.5 minutes at a current of 0.4 amps to attain the desired plating thickness. A similar calculation is made with copper except in order to determine its efficiency (usually between 10 and 60 percent), a trial plating procedure must be carried out for a timed period and the specimen's change in weight is recorded. Using the above relationship it is then possible to calculate the efficiency of the plating operation. The efficiency obtained in this experiment was determined to be 50 percent.

Besides using this calculational procedure to determine the weight of metal plated, the elbow is weighed before and after the electroplating process to insure an accurate measure of the depth of material plated. Below is the equipment list of apparatus used in

electroplating.

Equipment List:

1) Hallicrafters Model HP-1 Low Voltage Power Supply

2) Micronta Range Doubler Multitester - Cat. No. 22-204A

3) Corning Hot Plate-Stirrer PC-351.

APPENDIX D - Various Stages of Erosion of an Electroplated Elbow

The following photographs were taken during the course of the erosion of an electroplated elbow by 425 micron sand particles using a 35 mm camera.

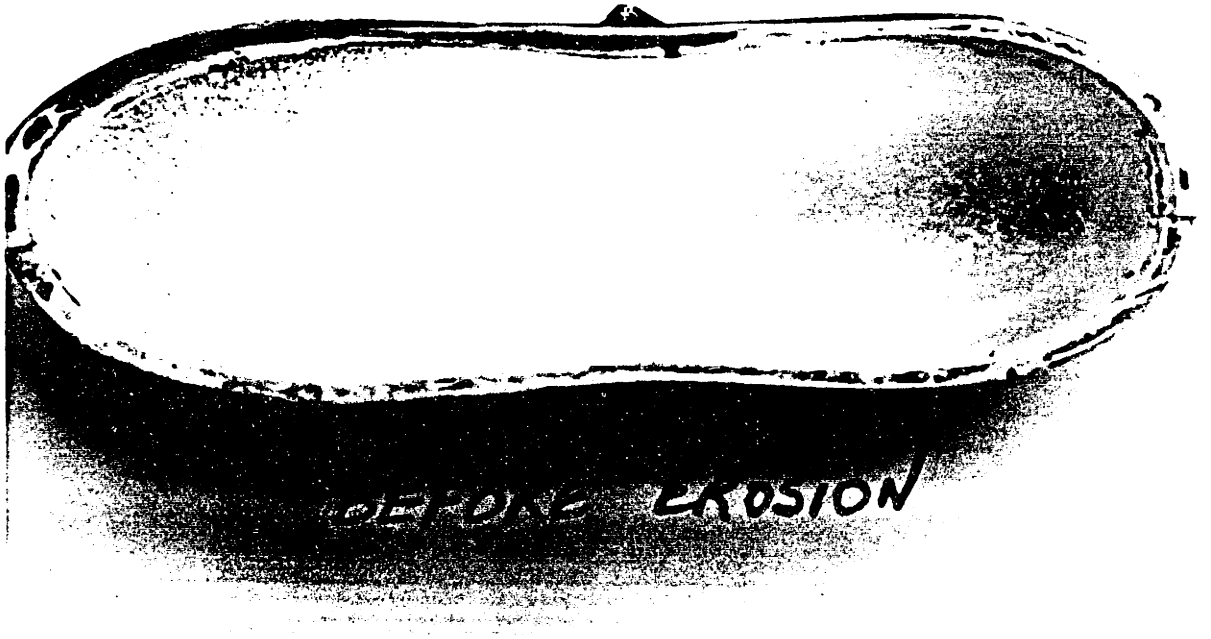

FIGURE 33 - SPECIMEN BEFORE EROSION

FIGURE 34 - AFTER 1.5 HOURS

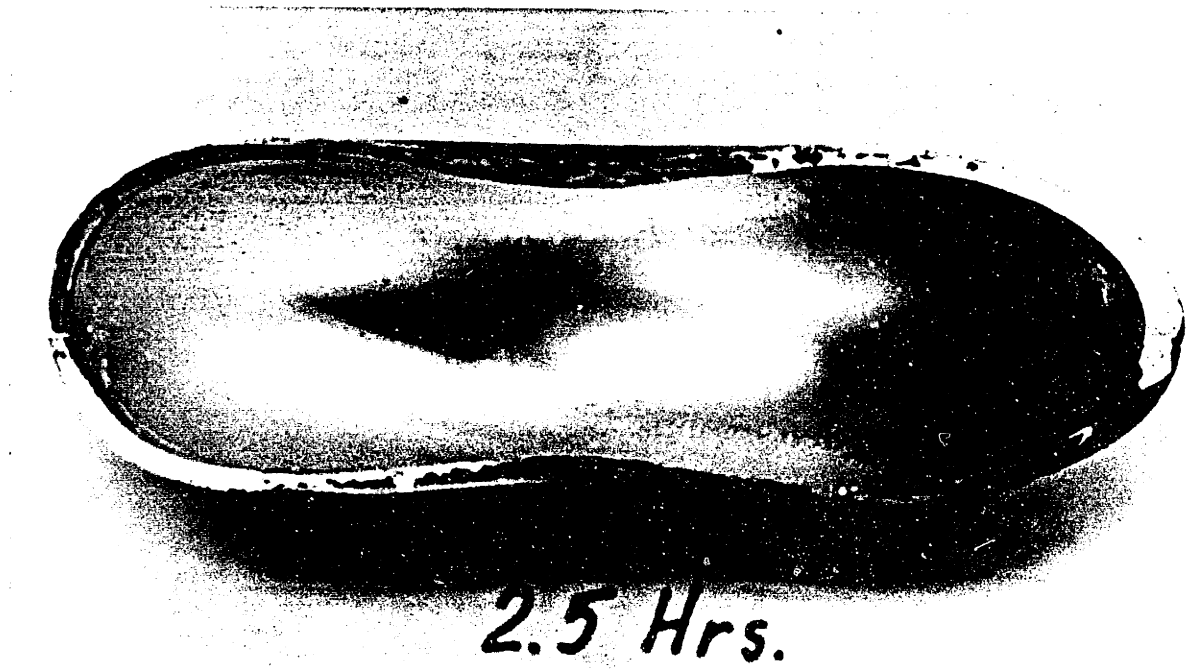

FIGURE 35 - AFTER 2.5 HOURS

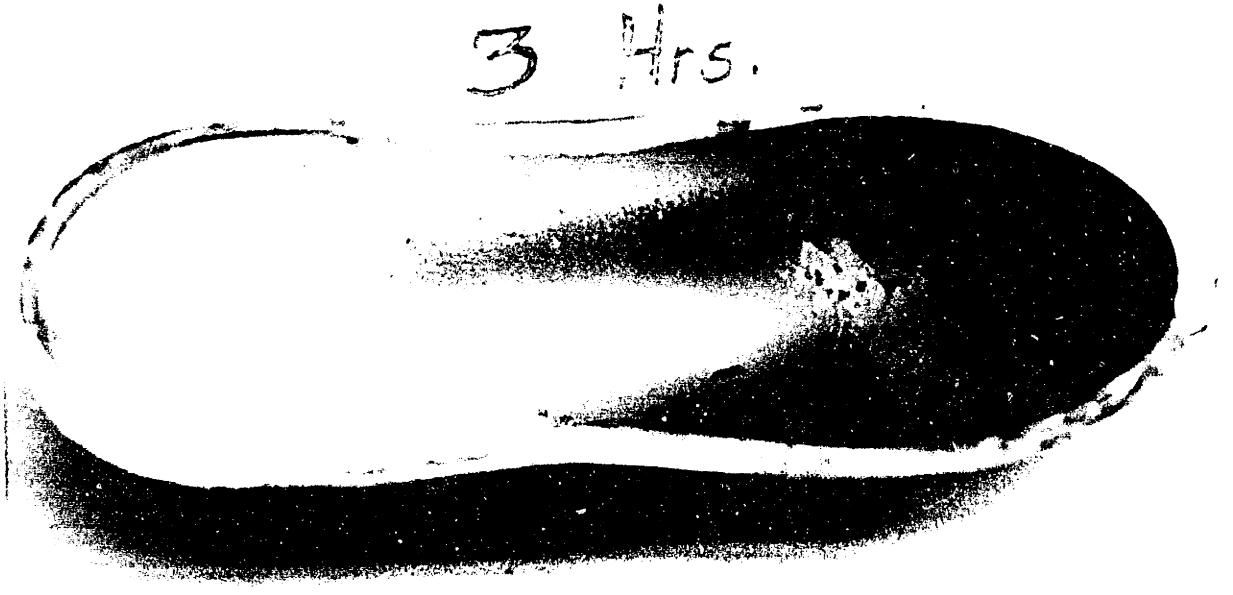

FIGURE 36 - AFTER 3 HOURS

FIGURE 37 - AFTER 4 HOURS

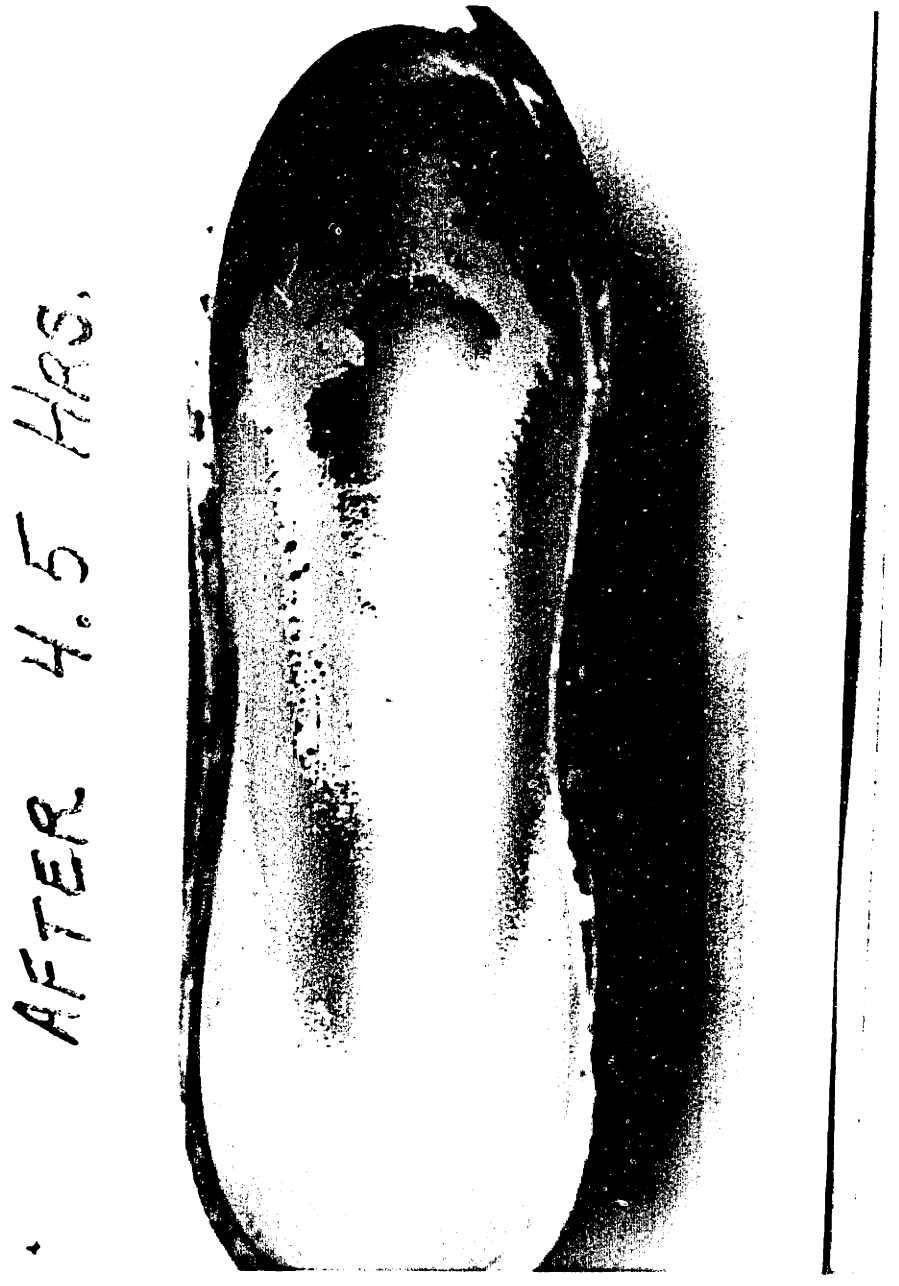

FIGURE 38 - AFTER 4.5 HOURS